Journal Pre-proofs

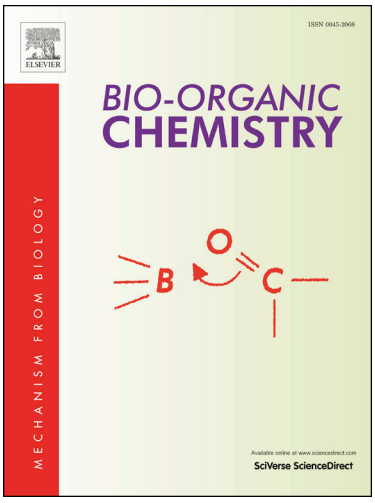

Inhibition of colitis by ring-modified analogues of 6-acetamido-2,4,5-trimethylpyridin-3-ol

Chhabi Lal Chaudhary, Prakash Chaudhary, Sadan Dahal, Dawon Bae, Tae-gyu Nam, Jung-Ae Kim, Byeong-Seon Jeong

PII: S0045-2068(20)31427-9
DOI: https://doi.org/10.1016/j.bioorg.2020.104130
Reference: YBIOO 104130

To appear in: *Bioorganic Chemistry*

Received Date: 10 April 2020
Revised Date: 2 July 2020
Accepted Date: 20 July 2020

Please cite this article as: C. Lal Chaudhary, P. Chaudhary, S. Dahal, D. Bae, T-g. Nam, J-A. Kim, B-S. Jeong, Inhibition of colitis by ring-modified analogues of 6-acetamido-2,4,5-trimethylpyridin-3-ol, *Bioorganic Chemistry* (2020), doi: https://doi.org/10.1016/j.bioorg.2020.104130

Title

Inhibition of colitis by ring-modified analogues of 6-acetamido-2,4,5-trimethylpyridin-3-ol

Author names and affiliations

Chhabi Lal Chaudhary[a], Prakash Chaudhary[a], Sadan Dahal[a], Dawon Bae[a], Tae-gyu Nam[b,]*, Jung-Ae Kim[a,]*, Byeong-Seon Jeong[a,]*

[a] *College of Pharmacy and Institute for Drug Research, Yeungnam University, Gyeongsan 38541, Republic of Korea*

[b] *Department of Pharmacy and Institute of Pharmaceutical Science and Technology, Hanyang University, Ansan, Gyeonggi-do 15588, Republic of Korea*

Corresponding authors

Byeong-Seon Jeong: Tel.: +82 53 810 2814; Fax: +82 53 810 4654; E-mail: jeongb@ynu.ac.kr

Jung-Ae Kim: Tel.: +82 53 810 2816; Fax: +82 53 810 4654; E-mail: jakim@yu.ac.kr

Tae-gyu Nam: Tel.: +82 31 400 5807; Fax: +82 31 400 5958; E-mail: tnam@hanyang.ac.kr

Highlights

- Ring-modified analogues of 6-acetamido-2,4,5-trimethylpyridin-3-ol were synthesized
- Structure-activity relationship of the ring-modified analogues were established
- Compound **17** inhibited TNF-α-induced responses in colonic epithelial cells better than tofacitinib
- Anti-colitis efficacy of compound **17** was much greater than tofacitinib in mice

Abstract

6-Aminopyridin-3-ol scaffold has shown an excellent anti-inflammatory bowel disease activity. Various analogues with the scaffold were synthesized in pursuit of the diversity of side chains tethering on the C(6)-position. Structure-activity relationship among the analogues was investigated to understand the effects of the side chains and their linkers on their anti-inflammatory activities. In this study, structural modification moved beyond side chains on the C(6)-position and reached to pyridine ring itself. It expedited us to synthesize diverse ring-modified analogues of a representative pyridine-3-ol, 6-acetamido-2,4,5-trimethylpyridin-3-ol (**9**). In the evaluation of compounds on their inhibitory actions against TNF-α-induced adhesion of monocytic cells to colonic epithelial cells, an *in vitro* model mimicking colon inflammation, the effects of compounds **9**, **17**, and **19** were greater than tofacitinib, an orally available anti-colitis drug, and compound **17** showed the greatest activity. In addition, TNF-α-induced angiogenesis, which permits more inflammatory cell migration into inflamed tissues, was significantly blocked by compounds **17** and **19** in a concentration-dependent manner. In the comparison of *in vivo* therapeutic effects of compounds **9**, **17**, and **19** on dextran sulfate sodium (DSS)-induced colitis in mice, compound **17** was the most potent and efficacious, and compound **19** was better than compound **9** which showed a similar degree of inhibitory effect to tofacitinib. Taken together, it seems that either the trimethyl system or the hydroxyl group on the pyridinol ring is essential to the activity. This finding might become a new milestone in the development of pyridinol-based anti-inflammatory bowel disease agents.

Graphical abstract

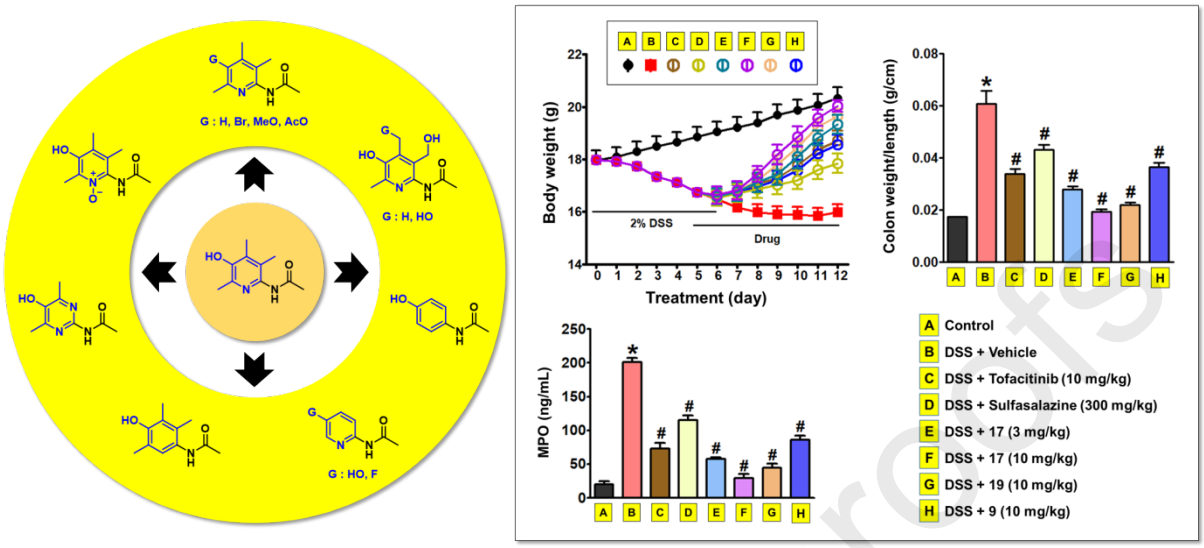

Keywords

Ring modification; 6-Aminopyridin-3-ol; Structure-activity relationship; TNF-α; Adhesion; Angiogenesis; Inflammatory bowel disease

1. Introduction

Inflammatory bowel disease (IBD) is a group of intestinal disorders that cause chronic relapsing inflammation of the gastrointestinal tract, with major subtypes of Crohn's disease (CD) and ulcerative colitis (UC) [1,2]. CD can occur throughout the gastrointestinal tract, from the mouth to the anus, and affects all layers of the intestinal wall [3]. UC typically occurs in the lower tract as the colon and rectum, and the area of injury usually begins in the rectum and can spread further through the colon [4]. Common symptoms of IBD are relapsing cycles of diarrhea, abdominal pain, rectal bleeding, bloody stools, weight loss, and fatigue. IBD, although known as a low mortality disease, severely impairs patients' quality of life. IBD is currently estimated to affect about 5 million people worldwide, including approximately 2.5 million people in Europe and 1.5 million in the United States, and is now rapidly spreading around the world [5].

The exact etiology of IBD is still incompletely understood, but it is commonly known to be caused by inappropriate immune responses to foreign organisms such as bacteria, viruses, or antigens in the intestinal tract in people with a genetic predisposition [6]. Defects of the intestinal mucosa and abnormalities of the innate immune system are considered to be the main causes of IBD, which interact to activate acquired immune T cells [7]. One that exists at the heart of this situation is the powerful inflammatory cytokine TNF-α (tumor necrosis factor-α). In relation to inflammation, TNF-α acts on vascular endothelial cells to induce angiogenesis [8] and promote more inflammatory cytokine secretion from macrophages [9]. In addition, it induces the death of intestinal epithelial cells [10], and activates MMPs of myofibroblasts to degrade the matrix [11] and promote the survival of Th17 cells [12]. Since the central role of TNF-α has been identified, anti-TNF-α monoclonal antibodies such as infliximab, adalimumab, and golimumab have been developed [13]. Due to the greater therapeutic efficacy of these antibody drugs than oral drugs such as salicylates, immunosuppressants, and corticosteroids,

these biologics play a major role in the treatment of IBD. However, such therapies using anti-TNF-α monoclonal antibodies are generally quite expensive and have the inconvenience of administration which must be given intravenously or subcutaneously. In addition, treatment failure, resistance, and side effects such as fluid reactions or infectious complications have been reported in many patients [14]. Regrettably, a considerable number of patients may fail to overcome IBD with anti-TNF-α biologics in the long run.

Consequently, there is an urgent need to develop new drugs that are more effective and safer than conventional ones. In particular, the development of small-molecule drugs of easier administration and lower cost compared to antibody biologics is also an important task to be achieved at the moment. Recently, several new small-molecule drugs have been developed and are currently being tested in phase II or III clinical trials [15–18]. The representative one is tofacitinib, a JAK (Janus kinase) inhibitor [19]. Tofacitinib has been used to treat rheumatoid arthritis since 2012. And it was approved for the treatment of adult patients in the United States with moderately to severely active UC in 2018 [20]. Although it is currently in phase II clinical trials for CD, it seems not effective for the treatment of CD [21,22].

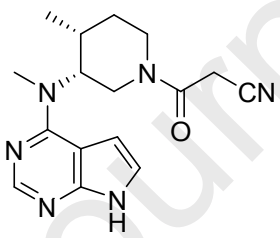

Tofacitinib

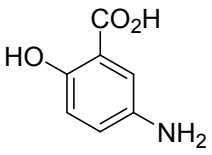

Mesalazine

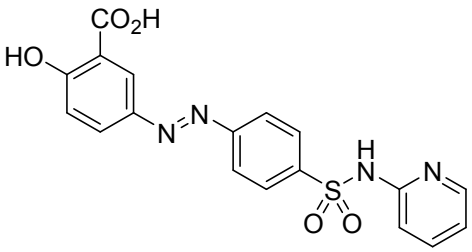

Sulfasalazine

A variety of molecular targets have been discussed due to the complex etiology and interactions between various cells in the study of IBD drug discovery [23], hence a strategy for new small-molecule drug discovery aiming only one target molecule may occasionally carry a risk of failure. In view of this point, we have established a cell-based in vitro screening system as a phenotype-based drug discovery strategy [24,25]. We set up an assay model that mimics tissue

damage caused by persistent influx of inflammatory cells such as monocytes, macrophages, and lymphocytes which are induced by TNF-α, a key factor in IBD pathogenesis. One characteristic occurrence observed in IBD is that inflammatory cells infiltrate and adhere to colon epithelium, which is induced by chiefly TNF-α. Treatment of colon epithelial cells with TNF-α leads to activation of NF-κB (nuclear factor κB), the most well-known transcription factor for up-regulating chemokines that recruit circulating leukocytes to the site of inflammation and adhesion molecules [26,27]. In the TNF-α-induced monocyte-epithelial cell adhesion assay system for quantification of inhibitory activity of test compounds against the adhesion process, colon epithelial cells (HT-29 cells) and monocytic cells (U937 cells) were co-cultured in the presence of TNF-α, and cell adhesion level was determined by measuring fluorescence signal subsequent to washing off unattached cells.

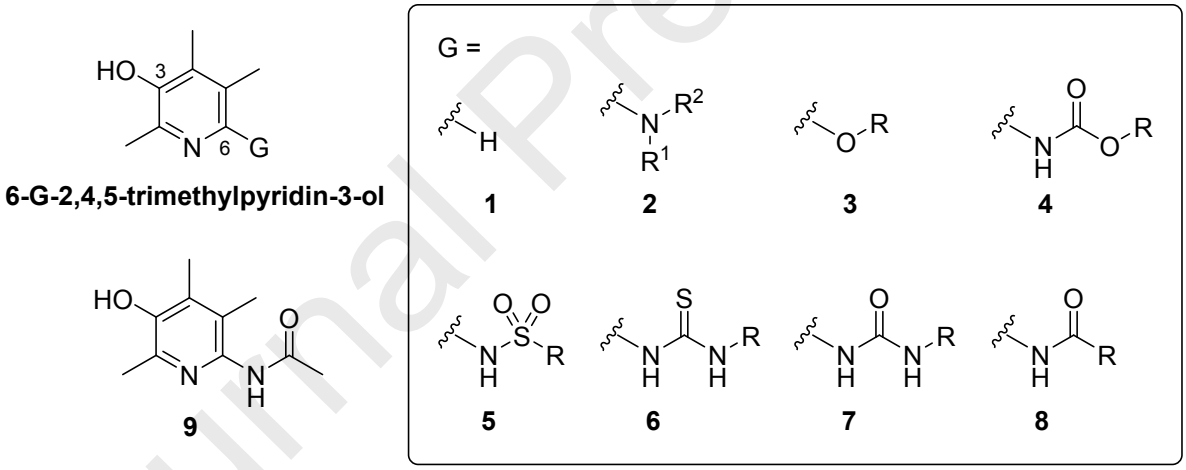

With this phenotype-based strategy using the in vitro assay as the primary screening system, we have been studying on the discovery of novel promising small-molecule compounds for the treatment of IBD for over a decade [28–35]. 2,4,5-Trimethylpyridin-3-ol (**1**) is the common skeleton of the compounds which we have been interested in and dealt with for this study so far [30,33,35–46]. We have prepared hundreds of its derivatives mostly by introducing several functional groups with various substituents at its C(6)-position, and are still designing and synthesizing new derivatives. From this 2,4,5-trimethylpyridin-3-ol library, we could pick out

some promising compounds that showed excellent efficacy against angiogenesis, cancers, or colitis, and so forth. Regarding IBD, we reported our findings in a series of papers to date on the 2,4,5-trimethylpyridin-3-ol derivatives with amino- (**2**), alkoxy- (**3**), carbamato- (**4**), sulfonamido- (**5**), thioureido- (**6**), or ureido- (**7**) functional groups [30,33,35]. We observed that these groups of compounds showed very potent inhibitory activity from the in vitro assays. Compared to mesalazine which is the active metabolite of the sulfasalazine (SSZ), a clinical drug for the treatment of IBD, they showed up to nearly 100,000 times better inhibition based on the IC_{50} values. Some compounds selected from the in vitro assay were subjected to *in vivo* experiments using acute colitis rat models, and all of the tested compounds administered were far superior to the positive control, SSZ.

Inflammatory cells including macrophages and mast cells can activate endothelial cells and proinflammatory cytokines produced from the cells such as TNF-α can induce angiogenesis, which recruits more inflammatory cells and worsens tissue damage [47]. Thalidomide, one of the old anti-TNF drugs, demonstrated to be effective in refractory pediatric IBD patients, and its effectiveness is known to be mediated through antiinflammatory and antiangiogenic effects [48]. Based on these reports, we have hypothesized that 6-amido-2,4,5-trimethylpyridin-3-ols (**8**) which were reported to show good antiangiogenic effects should have anti-IBD activity. Indeed, various amido compounds **8** clearly showed the activity (unpublished results). While those analogues have mainly featured structural variation on the C(6)-position, in this study, we aimed to investigate the effect of structural changes in the 2,4,5-trimethylpyridin-3-ol ring itself on the activity. For this purpose, we needed to fix C(6)-tethering group as acetamido group in order to reduce variables and grab clear idea on the structure-activity relationship (SAR). Compound **9** (6-acetamido-2,4,5-trimethylpyridin-3-ol) was considered a suitable reference for this study. Not only the acetamido group is the simplest amido-containing structure to provide us with convenient synthetic approaches but also acetamido-containing

compound **9** has an intermediate level of activity to afford us enough activity margin to explore a wider range of variation in activities that can be expected from new modifications.

2. Results and Discussion

2.1. Chemistry

To investigate the effect of pyridine ring on the activity, we have conducted ring modification in several different directions (Figure 1). The C(3)-OH group is either removed or blocked or replaced with other functional groups (compounds **10**, **12**, **17**, and **18**). Electron density of the pyridine ring was controlled as either N-oxide or pyrimidine/phenyl replacement (compounds **11**, **15**, and **16**). Trimethyl group on pyridine ring were either modified to hydroxymethyl group or removed (compounds **13**, **14**, and **19**). Detrimethyl analogue (compound **19**) was further modified to C(3)-F analogue or phenyl analogue (compounds **20** and **21**).

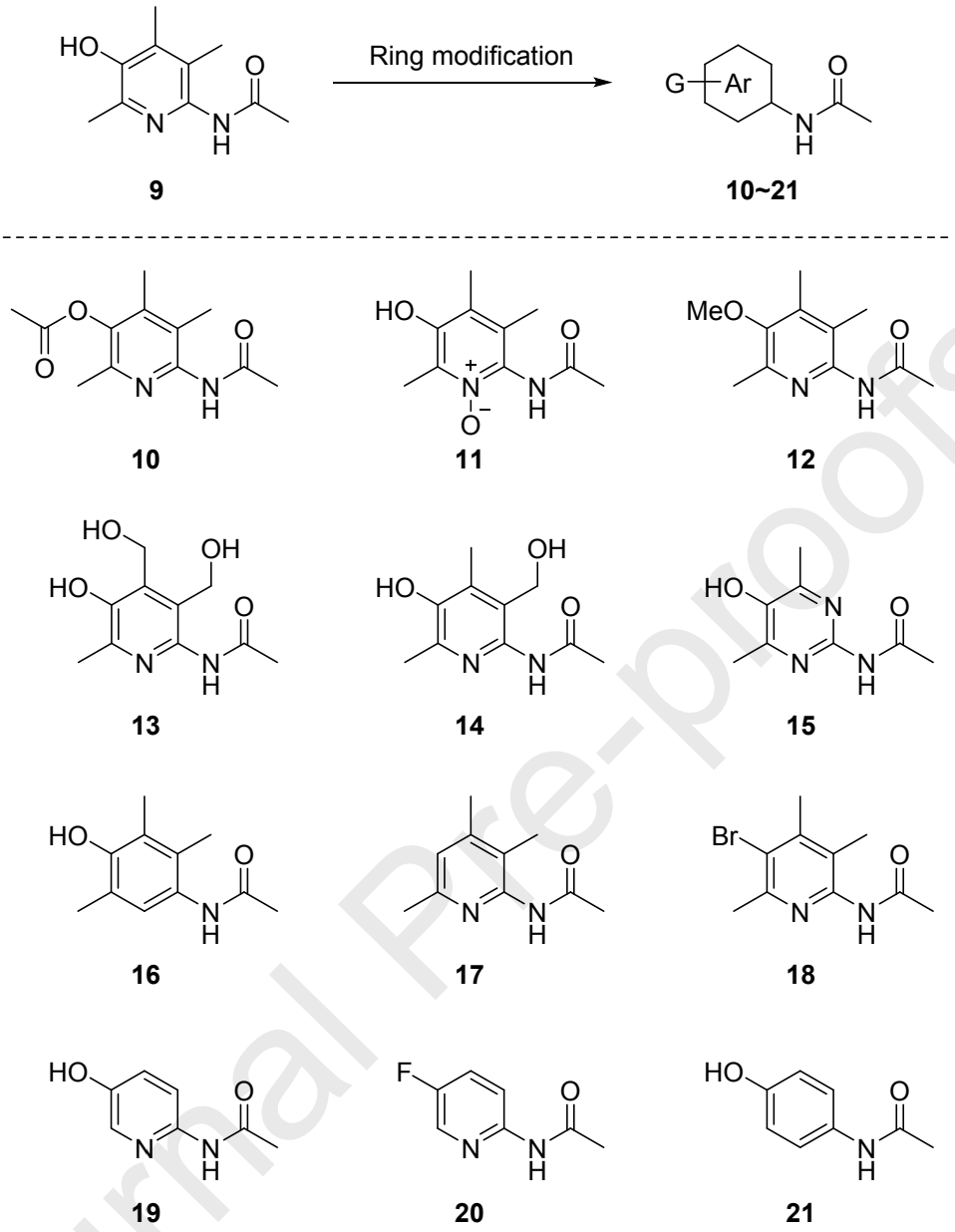

Figure 1.

As shown in Scheme 1, we synthesized the compounds **9** and **10** using the key intermediate **29,** which was obtained by the well-known route developed by us [38]. The synthesis started from inexpensive starting materials, pyridoxine hydrochloride (vitamin B_6, **22**). Firstly, the primary alcohols on **22** were converted to chlorines using a catalytic amount of DMF in $SOCl_2$. Secondly, the chlorines were reductively cleaved using Zn dust in acetic acid to obtain

trimethyl compound **24**. Then, the bromine at C(6)-position on **25** was introduced by electrophilic aromatic bromination reaction of **24** using 1,3-dibromo-5,5-dimethylhydantoin (DBDMH) and then the phenolic alcohol at C(3)-position was protected by benzyl bromide to give **26**. Next, the bromide of **26** was substituted by Buchwald-Hartwig amination with benzophenone imine to give imino-compound **27** followed by cleavage of the imine with methanolic HCl to give amino-compound **28**. Finally, the amino group in **28** was acetylated with acetyl chloride to afford **29**. The benzyl group of the intermediate **29** was deprotected to afford the compound **9** which was then acetylated again to afford methyl ester **10**.

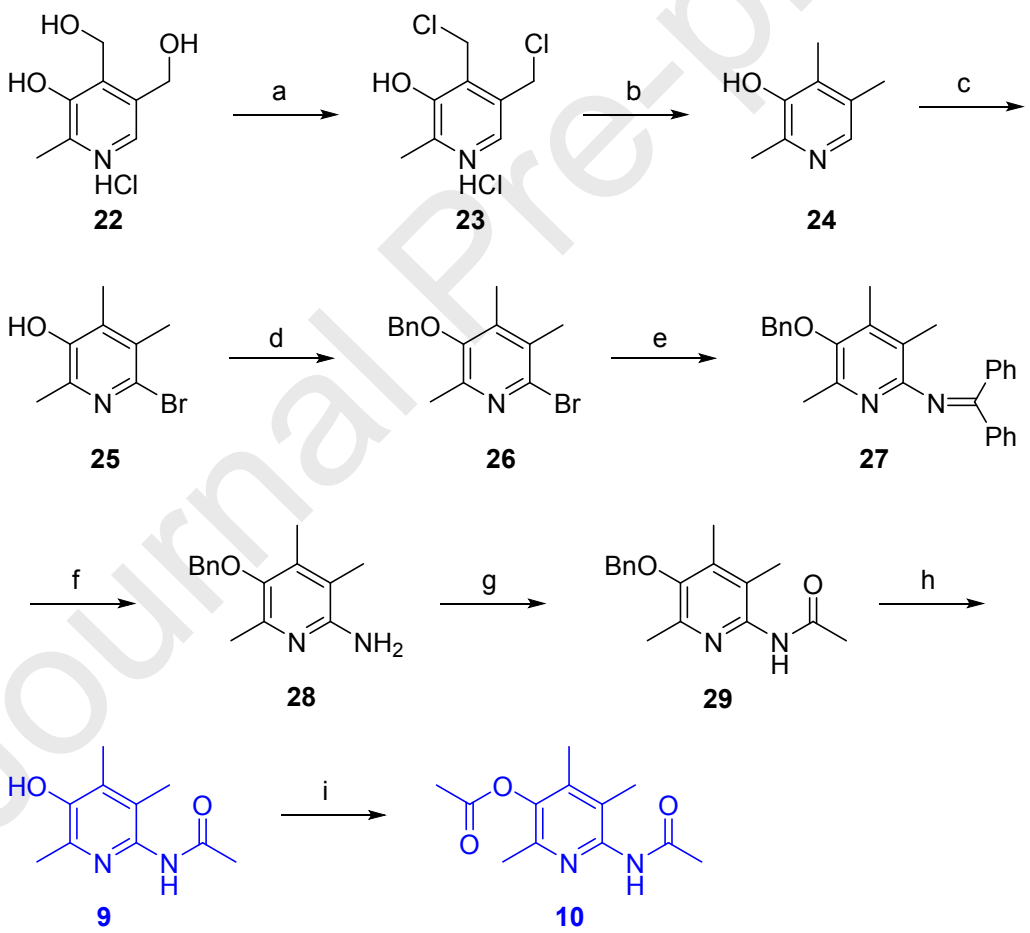

Scheme 1. *Reagents and Conditions*: (a) DMF, $SOCl_2$, 80 ℃, 4 h, 93%; (b) Zn, AcOH, 120 ℃, 4 h, 92%; (c) DBDMH, THF, r.t., 3 h, 70%; (d) $PhCH_2Br$, K_2CO_3, DMF, r.t., 12 h, 97%; (e) $Ph_2C{=}NH$, $Pd_2(dba)_3$, BINAP, NaO^tBu, PhMe, reflux, 6 h, 98%; (f) HCl/MeOH, THF, r.t., 1

h, 90%; (g) AcCl, NaOAc, Me_2CO, r.t., 4 h, 94%; (h) BCl_3, DCM, 0 ℃ to r.t., 2 h, 97%; (i) AcCl, NaOAc, Me_2CO, r.t., 3 h, 79%.

The direct synthesis of N-oxide analogue **11** from the compound **9** using *m*-CPBA or hydrogen peroxide was unsuccessful. Thus, the intermediate **29** was used as a starting substrate, as shown in Scheme 2. The intermediate **29** was treated with *m*-CPBA to give N-oxide compound **30** and was debenzylated by hydrogenolysis to afford compound **11**. Methoxy analogue **12** was synthesized *via* compound **33**. Previously, 3-methoxy-6-bromo-compound **31** was obtained by methylation of aromatic –OH of the 6-bromo compound **25** using iodomethane. Then, the amino compound **33** was obtained by Buchwald-Hartwig amination, followed by acidic methanolysis of the imine intermediate **32**, in two step sequences. The compound **33** was then acetylated to afford the acetamido compound **12** (Scheme 2).

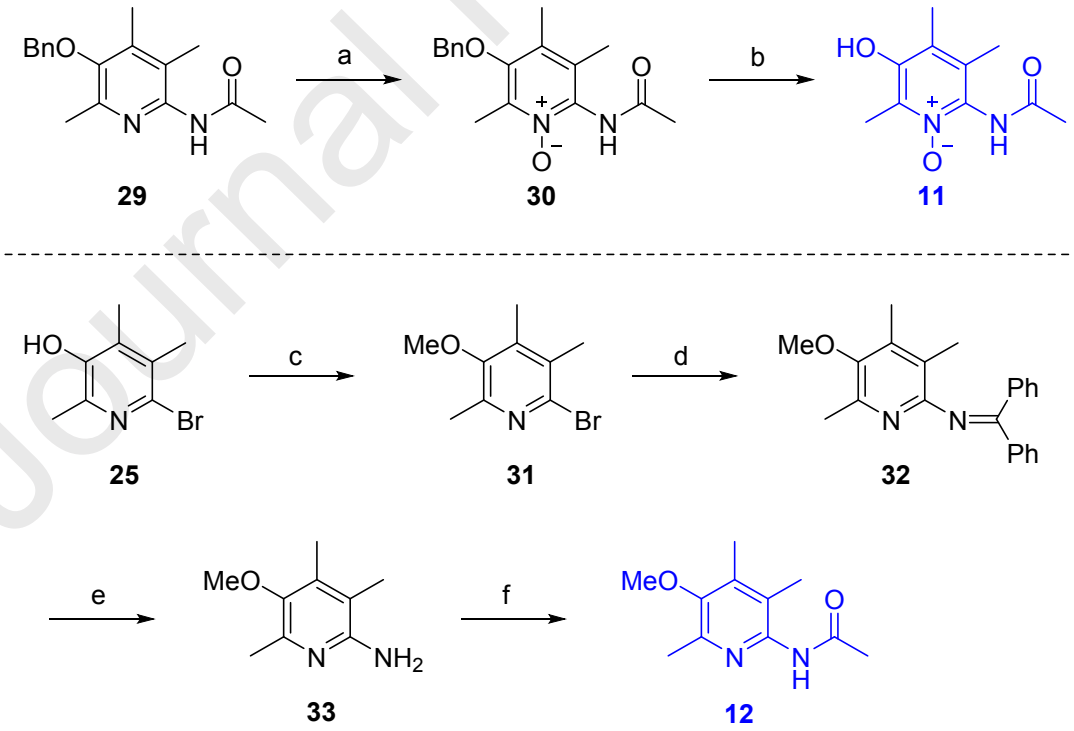

Scheme 2. *Reagents and Conditions*: (a) m-CPBA, $CHCl_3$, r.t., 30 min, 97%; (b) H_2, Pd/C,

MeOH, r.t., 1 h, 80%; (c) MeI, K_2CO_3, THF-H_2O (1:1), r.t., 21 h, 83%; (d) $Ph_2C{=}NH$, $Pd_2(dba)_3$, BINAP, NaO^tBu, PhMe, reflux, 6 h, 96%; (e) HCl/MeOH, THF-MeOH (1:1) , r.t., 2 h, 78%; (f) AcCl, Et_3N, DCM, r.t., 5 h, 73%.

The synthesis of hydroxylated analogues, **13** and **14**, are given in Scheme 3. 6-Aminopyridoxine hydrochloride (**35**) was synthesized by the reported procedure [49]. Pyridoxine hydrochloride (**22**) was reacted with diazotized aniline to afford 6-phenylazopyridoxine hydrochloride (**34**), which was then hydrogenated to yield amino compound **35**. Treatment of **35** with excess acetic anhydride in the presence of a catalytic amount of sulfuric acid produced the acetamide **13**. 6-Amino-4-dehydroxypyridoxine hydrochloride (**38**) was synthesized by the method reported by us [36,50]. Pyridoxine hydrochloride (**22**) was refluxed with Zn dust in acetic acid, followed by HCl in refluxing methanol gave 4'-dehydroxypyridoxine hydrochloride (**36**). The introduction of nitrogen moiety at C(6)-position of **36** was done by azo-coupling reaction with diazotized aniline to give azo-compound **37**. Azo bond was then cleaved by catalytic hydrogenolysis to afford amino-compound **38**. Finally, N-acetylation was carried out under the same reaction conditions as in the synthesis of **13** to obtain **14**.

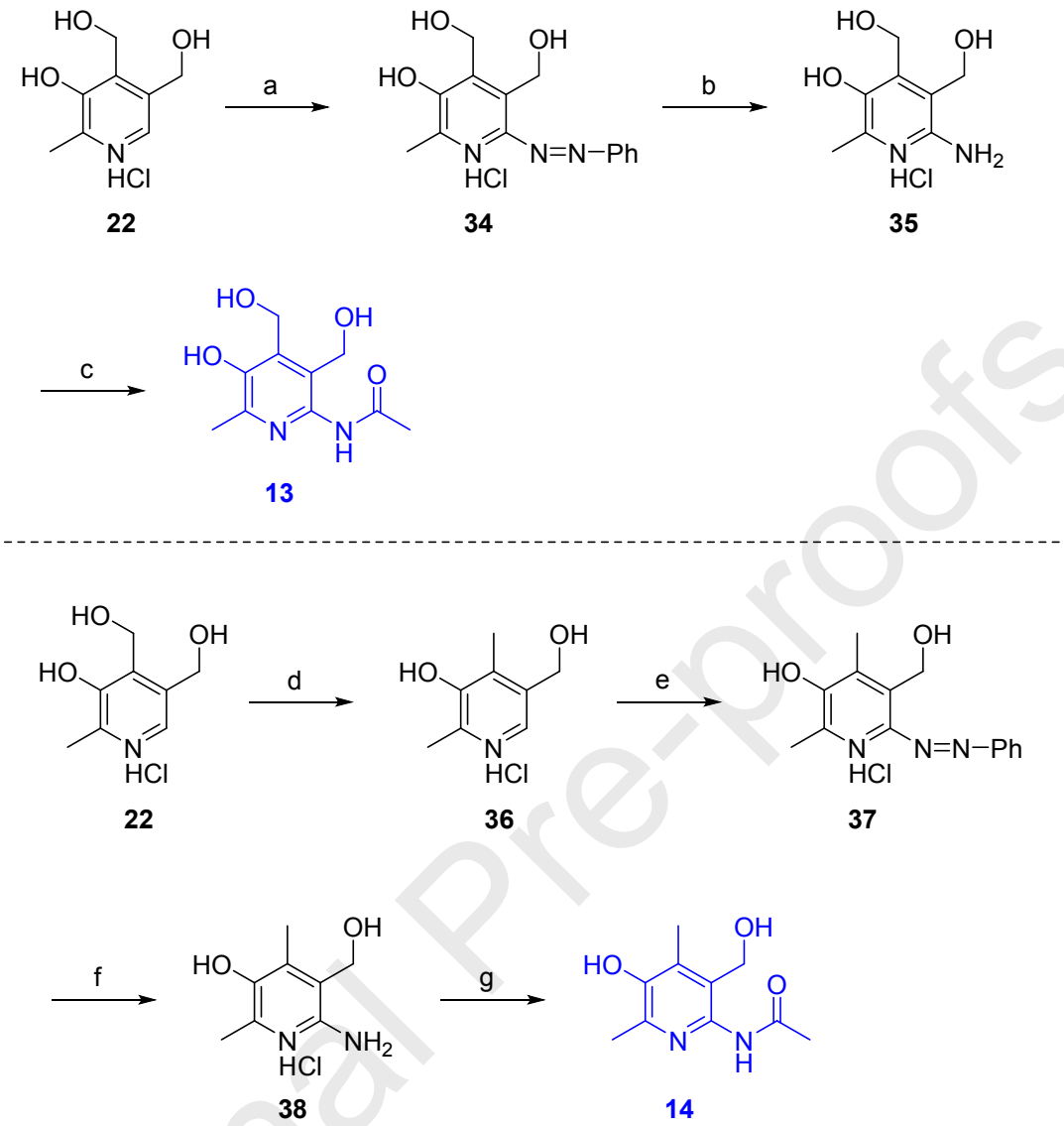

Scheme 3. *Reagents and Conditions*: (a) $PhNH_2$, $NaNO_2$, HCl, NaOH, H_2O, 0 ℃ to r.t., 1 h, 82%; (b) H_2, Pd/C, MeOH, r.t., 6 h, 45%; (c) Ac_2O, H_2SO_4, AcOH, 100 ℃, 30 min, 88%; (d) i) Zn, AcOH, 120 ℃, 3 h, ii) HCl/MeOH, MeOH, 60 ℃, 1 h, 93%; (e) $PhNH_2$, $NaNO_2$, HCl, NaOH, H_2O, 0 ℃ to r.t., 1 h, 95%; (f) H_2, Pd/C, MeOH, r.t., 6 h, 90%; (g) Ac_2O, H_2SO_4, AcOH, 100 ℃, 30 min, 48%.

Scheme 4 shows the synthesis of pyrimidine analogue **15** of the compound **9**. 5-Benzyloxy-4,6-dimethylpyrimidin-2-amine (**43**) was obtained by slight modification of the known procedures [51,52]. 2,4-Dioxopentan-3-yl acetate (**40**) was synthesized by replacement of

chloride in the compound **39** by acetate using a microwave reactor. 2-Amino-5-hydroxypyrimidine ring was formed by condensation reaction of **40** with guanidine (**41**) to give **42** which was further treated with benzyl chloride to get benzyloxy-compound **43**. Next, the 2-amino group was reacted with acetyl chloride to afford acetamido-compound **44**. Final debenzylation using BCl_3 provided the pyrimidine analogue **15**.

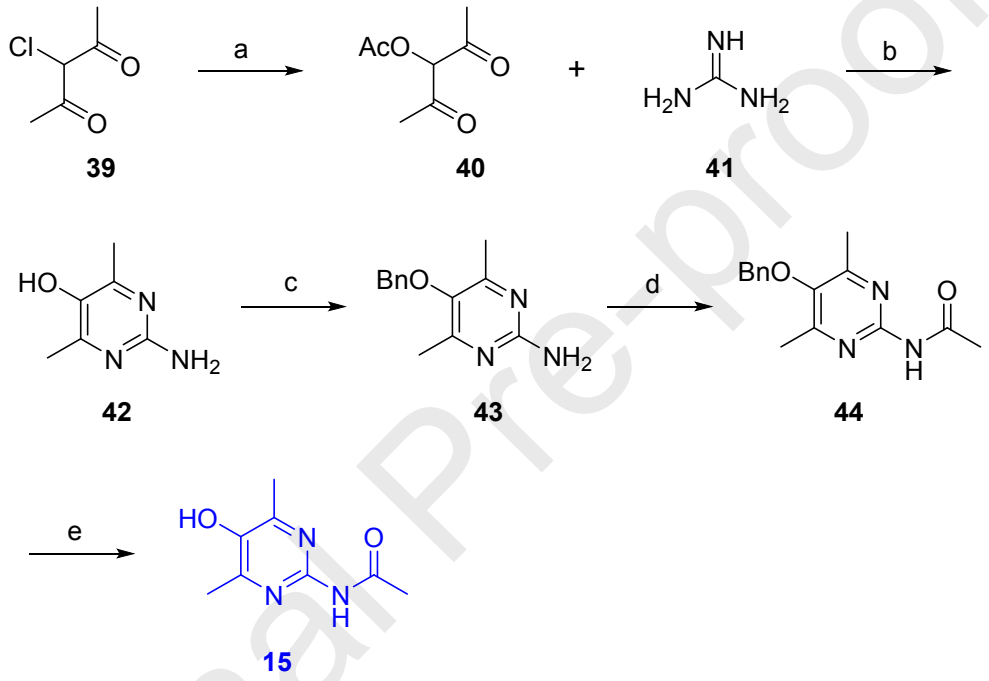

Scheme 4. *Reagents and Conditions*: (a) NaOAc, DMSO, MW, 50 ℃, 20 min; (b) NaOAc, DMSO, MW, 80 ℃, 30 min, 40% (2 steps); (c) $PhCH_2Cl$, NaOH, EtOH-DMF, 80 ℃, 12 h, 76%; (d) AcCl, Et_3N, DCM, r.t., 3 h, 39%, (e) BCl_3, C_6HMe_5, DCM, r.t., 30 min, 49%.

The phenyl analogue **16** of the compound **9** was prepared starting from a hydroquinone **45** as shown in Scheme 5. 2,3,5-Trimethylbenzene-1,4-diol (**45**) was oxidized to 1,4-benzoquinone **46** and then converted to mono-oxime compound **47** using hydroxylamine·HCl. Mono-oxime formation has been known to be selective to the steric environment of carbonyl moiety in quinone system [53]. Of course, in the compound **46**, the less hindered carbonyl was the

primary site for the reaction. Reduction of the compound **47** with $SnCl_2$ gave *p*-aminophenol compound **48** which was finally treated with acetyl chloride to afford **16**.

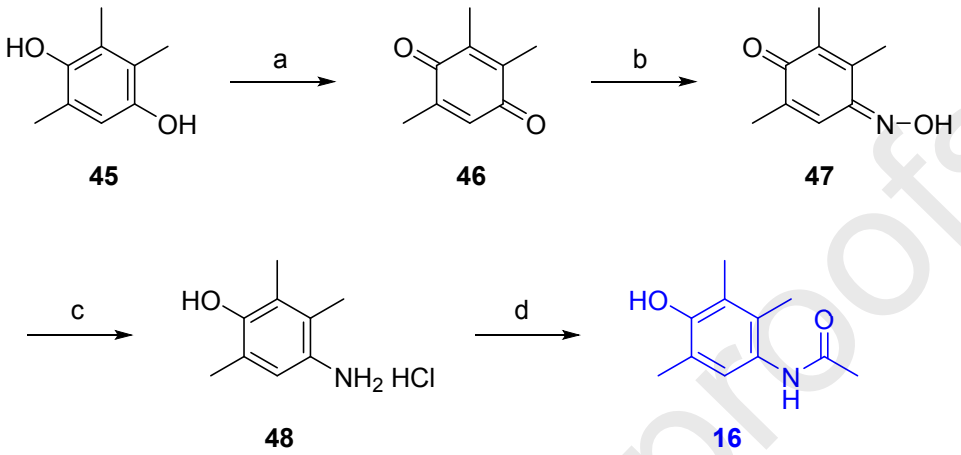

Scheme 5. *Reagents and Conditions*: (a) $PhI(OAc)_2$, MeOH, r.t., 1 h; (b) NH_2OH•HCl, THF, reflux, 2 d, 72% (2 steps); (c) $SnCl_2$, HCl, DCM, r.t., 2 h, 32%; (d) AcCl, NaOAc, Me_2CO, r.t., 3 h, 41%.

The synthesis of dehydroxylated analogue **17** of the compound **9** was shown in Scheme 6. This synthetic strategy was designed based on the known procedure on phenolic C–O bond cleavage [54]. The 6-bromopyridin-3-ol **25** was taken as the starting material and reacted with 5-chloro-1-phenyltetrazole (**49**), the key reagent for this synthesis, to give **50**. Amino group was introduced by the two sequential reactions; imination under the Buchwald-Hartwig conditions to give **51**, and cleavage of the imine under acidic methanolysis conditions to give **52**. Then, hydrogenolysis of the phenolic C–O bond in **52** gave the deoxygenated product **53** which was then acetylated to afford the final compound **17**, the deoxy-analogue of **9**. For the 3-bromo analogue **18**, two-step procedure was needed from the intermediate **53**; bromination and acetylation.

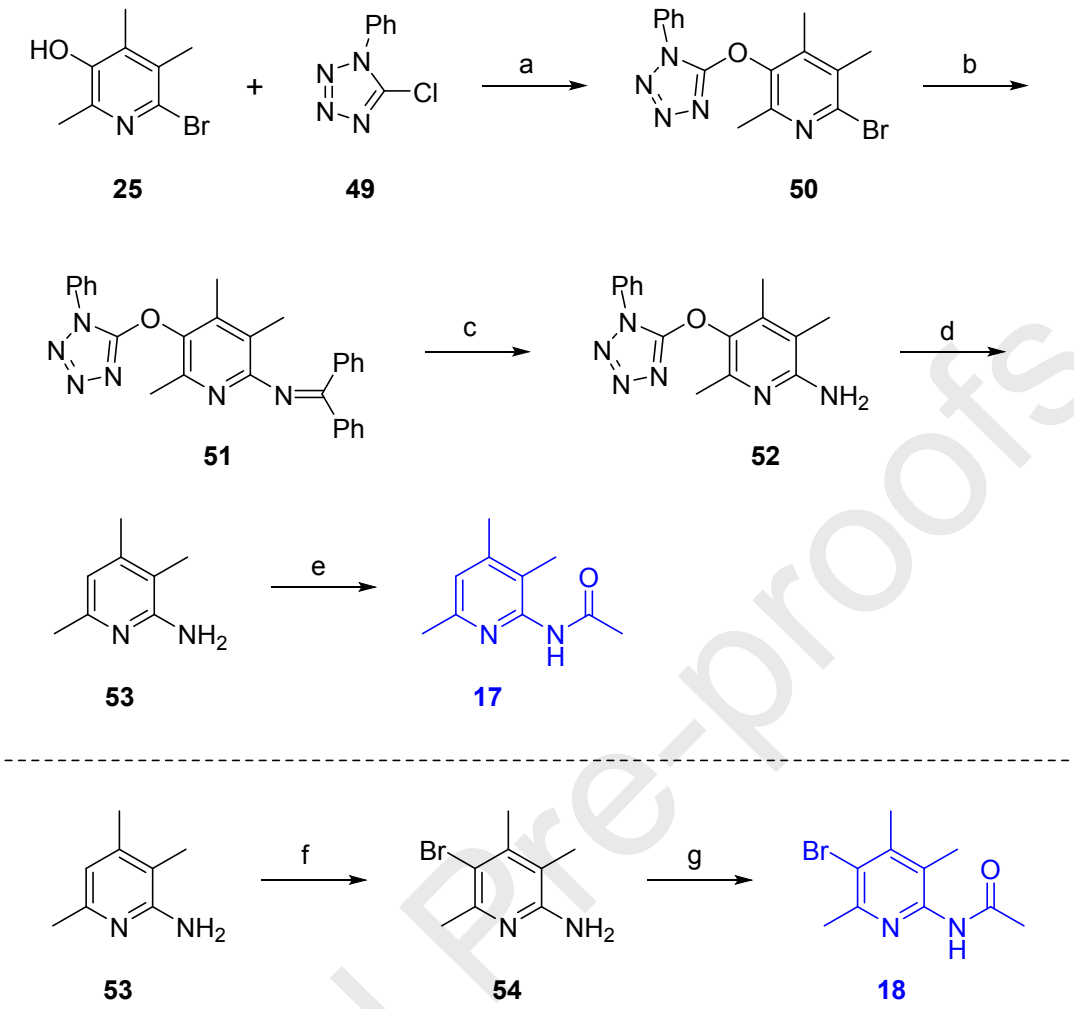

Scheme 6. *Reagents and Conditions*: (a) NaOH, MeCN, MW, 200W, 100 ℃, 1 h, 92%; (b) Ph_2C=NH, $Pd_2(dba)_3$, BINAP, NaO^{t}Bu, PhMe, reflux, 3 h; (c) HCl/MeOH, MeOH-THF (1:1), r.t., 3 h, 70% (2 steps); (d) H_2, Pd/C, MeOH, r.t., 3 d, 51%; (e) AcCl, NaOAc, Me_2CO, r.t., 4 h, 25%; (f) NBS, NH_4OAc, MeCN, r.t., 10 min, 41%; (g) AcCl, Et_3N, Me_2CO, r.t., 24 h, 47%.

For the demethylated analogue **19** of the compound **9**, synthesis started from 3-hydroxypyridine (**25**) which was treated with diazotized *p*-nitroaniline (**55**) to give azo-compound **56**. After cleavage of azo bond affording **57**, acetylation finally gave **19** [55]. Similarly, commercially available 5-fluoropyridin-2-amine (**58**) was simply acetylated to give 3-fluoro-demethylated analogue **20**. The demethyl-phenyl analogue **21** (paracetamol) was purchased. (Scheme 7)

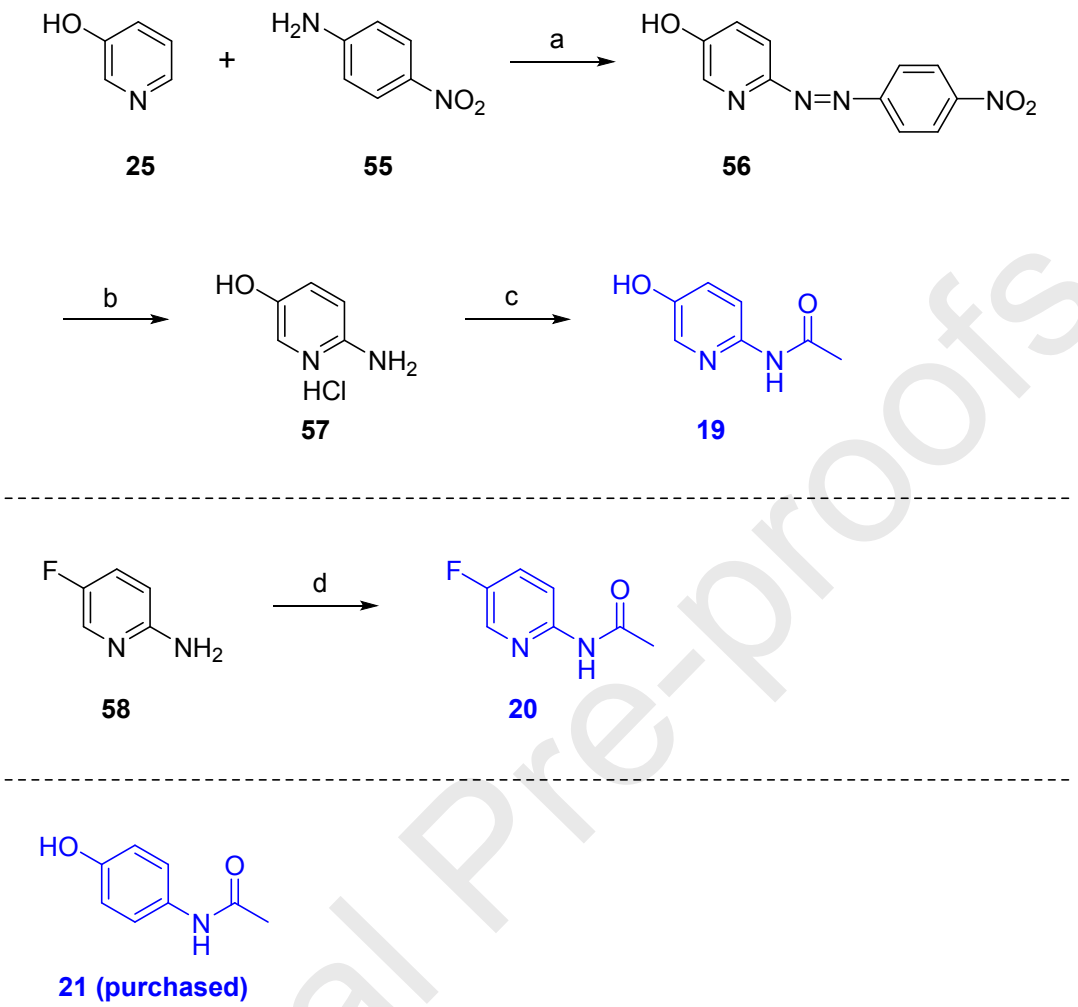

Scheme 7. *Reagents and Conditions*: (a) $NaNO_2$, HCl, NaOH, H_2O, r.t., 1.5 h, 96%; (b) H_2, Pd/C, MeOH, r.t., 12 h, 64%; (c) i) AcCl, Et_3N, DCM, r.t., 3 h, ii) NaOH, H_2O, r.t., 30 min, 30%; (d) AcCl, NaOAc, Me_2CO, r.t., 30 min, 38%.

2.2. Biology

Inhibitory activity of the compounds against TNF-α-induced cell adhesion is summarized in Table 1. Compound **9** is the parent compound on which ring modification was conducted to prepare the analogues **10**–**21**. First, we investigated the effect of modification in electron density of the pyridine ring on the inhibitory activity. A parent compound **9** showed 56% inhibition which is almost similar to tofacitinib, a positive control and JAK/STAT inhibitor,

and tremendously higher than mesalazine, an approved drug for IBD. Its direct phenyl analogue **16** significantly lost the activity indicating that the absence of nitrogen atom in pyridine ring leading to increase some degree of electron density, decreased adhesion-inhibitory activity. However, decrease in electron density of the pyridine ring of **9** in a form of N-oxide **11** and pyrimidine **15** also resulted in decrease of the biological activity. Such discrepancy between electron density and the activity imply that other factors, e.g., steric factor also contribute the activity. Removal of the trimethyl groups on pyridine ring of **9** resulted in astonishing increase in the adhesion-inhibitory activity (69.5%, **19**). Further removal of nitrogen from pyridine ring decreased the activity (21.4%, **21**, paracetamol, an antipyretic analgesic drug). Such decrease by 48.1% (**19** vs. **21**) was comparable to 44.6% decrease (**9** vs. **16**) which are commonly reflected by the absence of pyridine ring nitrogen. As for steric factors, shrunk steric bulkiness in **19**, compared to **9**, significantly increased the activity while removal of ring nitrogen as in **16** resulted in dramatic reduction in the activity, compared to **9**. Modification of trimethyl groups into hydroxymethyl groups afforded two analogues, **13** and **14**. The former has hydroxymethyl groups both on C(3)- and C(4)-positions to cause quite a decrease in activity, compared to **9**, while installation of hydroxymethyl group only in C(3)-position (**14**) restored the activity to almost comparable level to **9**. Next, role of C(3)-OH group on the activity was investigated. Acetyl capping on C(3)-OH group of **9** afforded the slight loss of the activity (**10**). Both methyl capping and the replacement of C(3)-OH group with bromide resulted in almost the same degree of decrease (**12** and **18**, respectively). Surprisingly, removal of C(3)-OH group afforded increase in the activity to considerable extent (77.6%, **17**). It is indicated that either an intact hydroxy group or a hydrogen should be attached on C(3)-position for the maximum activity. Besides, replacement of C(3)-OH group of **19** which showed a high adhesion-inhibitory activity (69.5%) with fluoride (**20**) again resulted in decrease in the activity. It is noteworthy that **17** (dehydroxylated analogue of **9**) and **19** (detrimethylated version of **9**)

showed comparable activities (77.6% and 69.5%, respectively) which are higher than **9**. Taken together, it is suggested that either C(3)-OH group or trimethyl group is essential for the activity individually and both functional groups decreased the activity a bit when installed together. Mechanistically, cell adhesion assay in this report is not based on a specific target but only observed TNF-α-induced adhesion as a phenotypic experiment. It is unclear at this point if our compounds inhibited the interaction between TNF-α and its receptor on the cell surface or penetrated cell membrane to inhibit cell adhesion *via* intracellular mechanism. One of the reliable predictions for cell permeability is the Lipinski's rule of five for drug-likeness. It indicates that logP should not exceed 5 in order not to be too lipophilic. Calculated logP (cLogP) values of test compounds range from –1.098 to 1.728 except for 2.267 for compound **18**. Therefore they conform to the Lipinski's rule and can be expected to possibly cross cell membrane. On the other hand, their low cLogP values also indicate that they are quite polar and their permeability will be limited to some extent.

Table 1. Inhibitory activity against TNF-α-induced adhesion of human monocytic cells (U937) to human colonic epithelial cells (HT-29).

Compound	Concentration	% Inhibition[a]	IC_{50}
9	1 μM	56.0 ± 6.3*	0.70 ± 0.10 μM
10	1 μM	39.5 ± 2.8*	n/a[b]
11	1 μM	21.9 ± 4.9*	n/a[b]
12	1 μM	34.7 ± 6.5*	n/a[b]
13	1 μM	16.0 ± 2.3*	n/a[b]
14	1 μM	51.8 ± 4.3*	n/a[b]
15	1 μM	28.8 ± 4.2*	n/a[b]
16	1 μM	11.4 ± 5.8	n/a[b]

17	1 μM	77.6 ± 4.7*	0.32 ± 0.10 μM
18	1 μM	37.2 ± 5.5*	n/a[b]
19	1 μM	69.5 ± 4.3*	0.48 ± 0.14 μM
20	1 μM	20.3 ± 7.0	n/a[b]
21 (Paracetamol)	1 μM	21.4 ± 5.3	n/a[b]
Tofacitinib	1 μM	50.8 ± 3.9*	0.71 ± 0.10 μM
Mesalazine	10,000 μM	37.3 ± 3.3*	21.34 ± 2.28 mM

[a] Data are shown as 'mean ± SEM' of at least three independent experiments performed in triplicate.

*P <0.05 versus vehicle-treated group.

[b] n/a: not applicable

To determine cytotoxicity of compounds **9**, **17**, and **19**, we compared the effects of the compounds, tofacitinib and mesalazine on the viability of CCD-841 normal human colon epithelial cells. Tofacitinib significantly decreased the viability of CCD-841 in a concentration-dependent manner (Figure 2). However, compounds **17** and **19** were much less cytotoxic than tofacitinib, while mesalazine was much safer than **17** and **19** in CCD-841 cells (Figure 2).

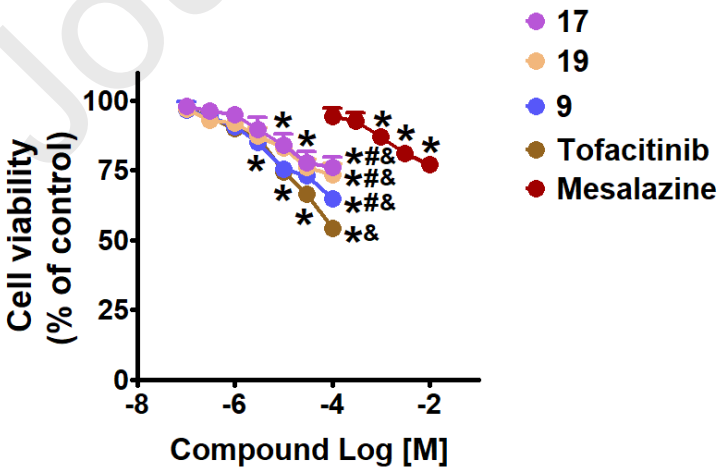

Figure 2. Cytotoxic effects of the selected compounds (**9**, **17** and **19**), tofacitinib, and mesalazine on the viability of CCD-841 normal human colon epithelial cells. Results are presented as the mean ± SEM of three independent experiments. *P < 0.05 versus vehicle-treated controls. $^{\#}P < 0.05$ versus tofacitinib-treated group. $^{\&}P < 0.05$ versus mesalazine-treated group.

Although the effect of TNF-α on angiogenesis is controversial, temporal expression of TNF-α is important for induction of angiogenesis. Continuously exposed to TNF-α, endothelial cells are sprouting and undergo angiogenesis [56], which resembles the relapsing event of inflammation in IBD condition. Based on these notion, we examined inhibitory actions of the effective compounds on TNF-α-induced angiogenesis. In an *in vivo* angiogenesis assay using chick chorioallantoic membrane (CAM) in which newly formed vessel branch points were counted, an angiogenic ability of TNF-α was comparable to that of vascular endothelial growth factor (VEGF) (Figure 3). Compounds **17** and **19** significantly inhibited TNF-α-induced angiogenesis in a concentration-dependent manner up to the vehicle-treated controls (Figure 3).

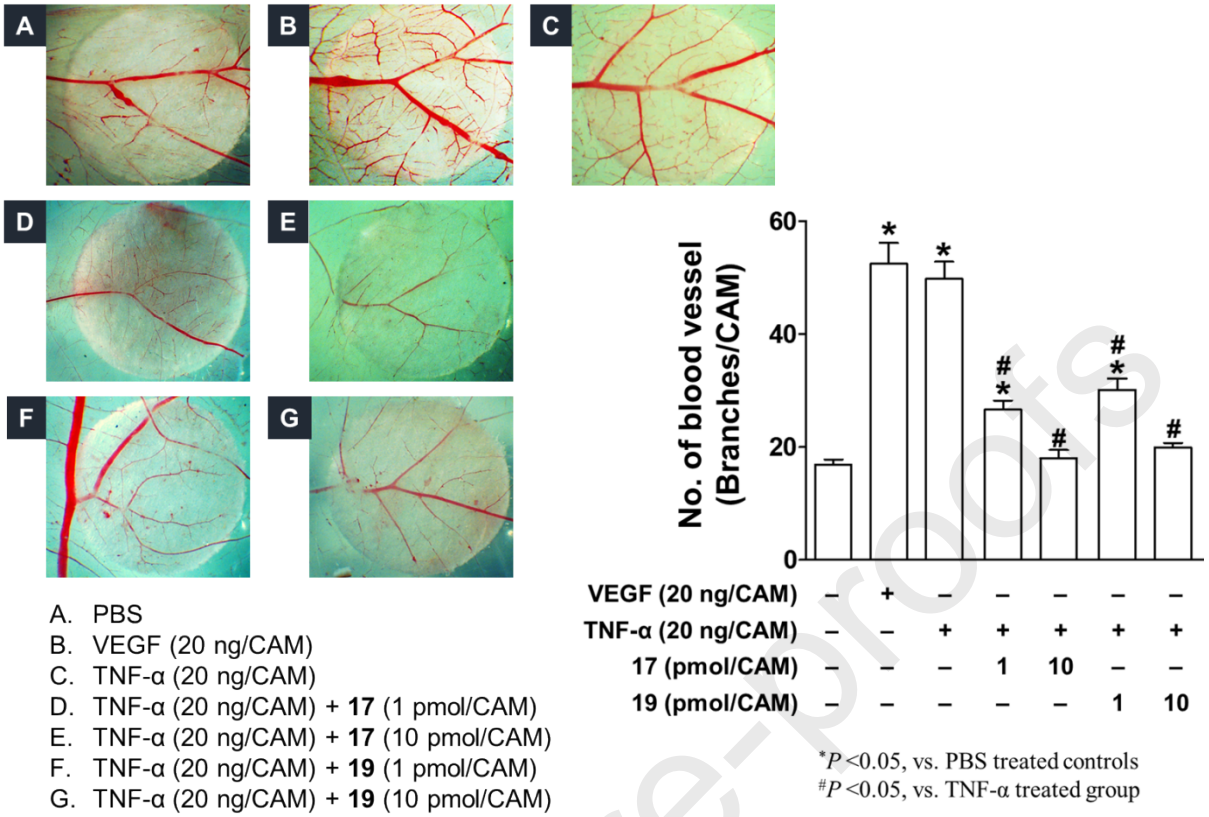

Figure 3. Inhibitory effects of the selected compounds (**17** and **19**) on TNF-α-induced angiogenesis of CAM as an in vivo model (n = 8).

a

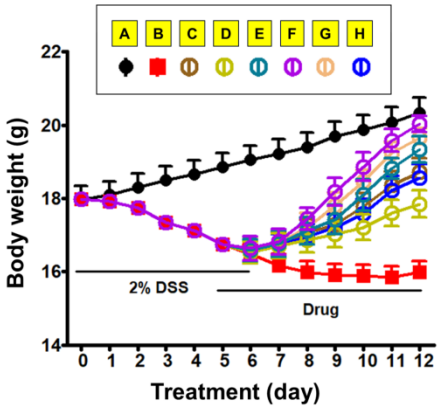

Body weight recovery			
Compound	Dose (mg/kg)	Admin.	Recovery (%) (Mean ± SEM)
Tofacitinib	10	IP	62.7 ± 8.8
Sulfasalazine	300	PO	42.9 ± 8.5
17	3	IP	76.8 ± 8.2
17	10	IP	93.1 ± 5.1
19	10	IP	84.4 ± 5.9
9	10	IP	58.9 ± 8.6

b

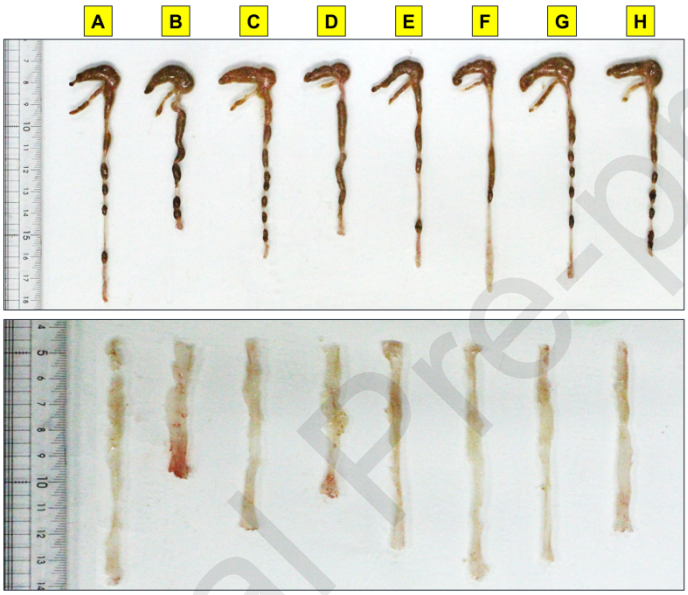

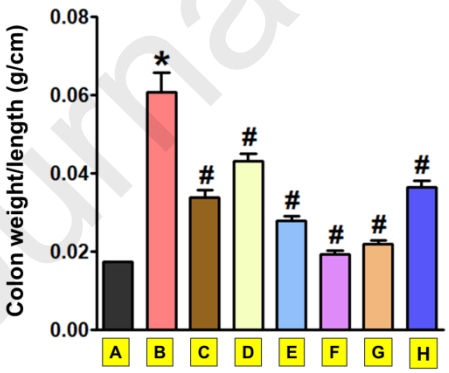

Colon weight/length recovery			
Compound	Dose (mg/kg)	Admin.	Recovery (%) (Mean ± SEM)
Tofacitinib	10	IP	61.9 ± 3.6
Sulfasalazine	300	PO	41.0 ± 4.2
17	3	IP	76.5 ± 2.3
17	10	IP	95.2 ± 1.9
19	10	IP	87.7 ± 2.8
9	10	IP	57.4 ± 3.5

c

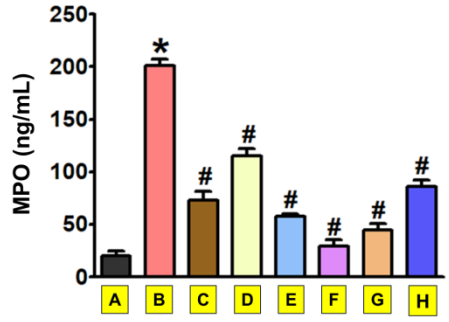

- A Control
- B DSS + Vehicle
- C DSS + Tofacitinib (10 mg/kg, IP)
- D DSS + Sulfasalazine (300 mg/kg, PO)
- E DSS + 17 (3 mg/kg, IP)
- F DSS + 17 (10 mg/kg, IP)
- G DSS + 19 (10 mg/kg, IP)
- H DSS + 9 (10 mg/kg, IP)

Figure 4. Compounds **9**, **17** and **19** ameliorates the clinical features of DSS-induced colitis in mice (n = 5). Colitis was induced by oral administration of DSS dissolved in drinking water. Data represent the mean ± SEM for five mice per group. *$P < 0.05$ versus vehicle-treated control group. $^{\#}P < 0.05$ versus vehicle-treated DSS group.

Next, we examined ameliorating effects of compounds **17** and **19** together with **9** on dextran sulfate sodium (DSS)-induced colitis in mice. To compare therapeutic effects, compounds were administered after mice were given DSS treatment over five consecutive days. DSS treatment resulted in the development of colitis assessed by decrease in body weight (Figure 4a) and increases in colon-weight/unit-length (Figure 4b) and levels of myeloperoxidase (MPO) levels, a biochemical marker of colon tissue inflammation (Figure 4c). Because the purpose of this study is to confirm the efficacy *in vivo*, the test compounds were administered intraperitoneally (IP) to bypass the first-pass effect accompanied by oral administration (PO). Although tofacitinib is an orally available drug, it was administered both IP and PO as a positive control. Compound **17** with the best *in vitro* effect which was administered intraperitoneally at two doses, 3 and 10 mg/kg significantly blocked colitis and showed a recovery rate of 93% at 10 mg/kg dose. At 10 mg/kg dose, **19** was less effective than **17**, but much greater than tofacitinib and **9**. Anti-colitis effects of all compounds were greater than sulfasalazine (300 mg/kg) which was orally administered to mice. When DSS (2w/v%) treatment was extended one more day (total 7 days), body weight reduction was much greater than 6-day treatment, indicating 7-day DSS treatment induced much more severe colitis in mice (Figure 4a *vs.* Figure 5a). The mice treated with DSS alone became very weak resulting in more than half (67%) of mice not surviving by the end point. Administration of SSZ (300 mg/kg, PO), tofacitinib (10 mg/kg, IP and 30 mg/kg, PO), and compound **9** (10 mg/kg, IP) did not restore body weight significantly (Figure 5a). Particularly, treatment with tofacitinib (IP, 10 mg/kg) caused DSS-induced death

at earlier time point than the vehicle-treated group (Figure 5b), and tofacitinib PO (30 mg/kg) administration group showed a higher DSS-induced mortality rate than the IP (10 mg/kg) administration group. However, compound **17** significantly recovered body weight at 4 days after administration, and the recovery effect was dose-dependent (Figure 5a).

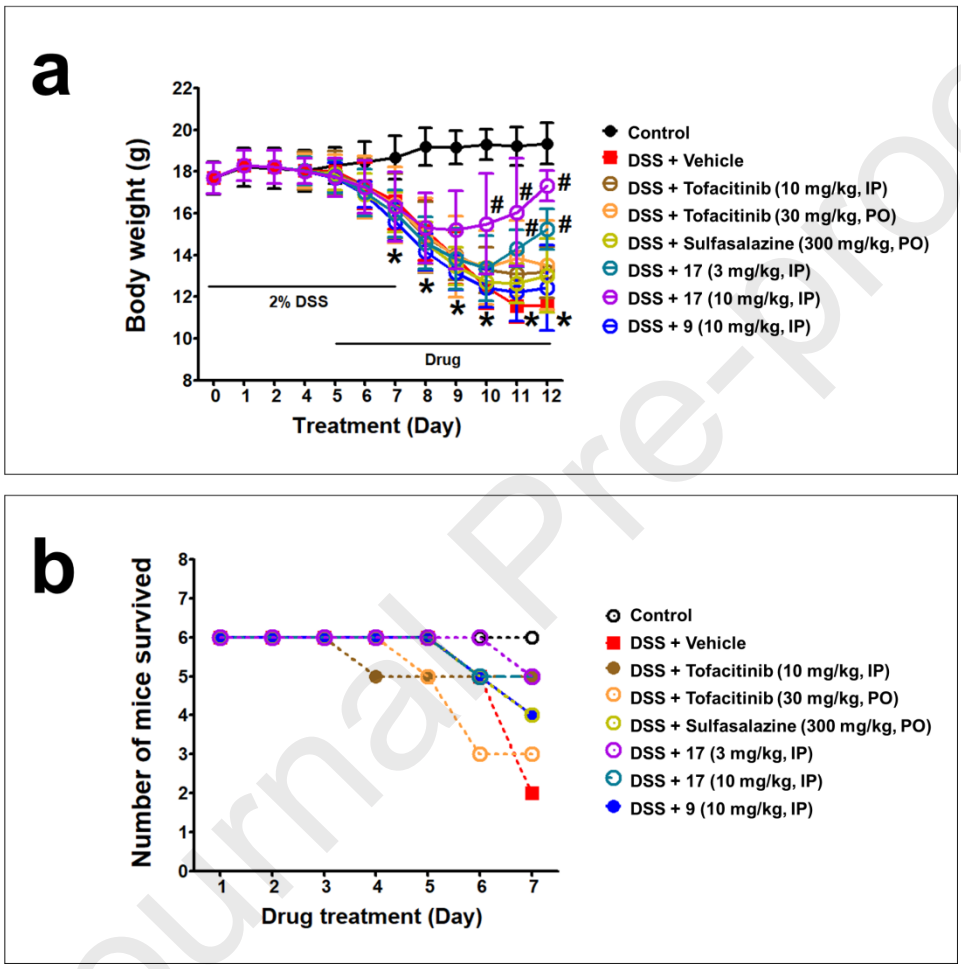

Figure 5. Compound **17** ameliorates severe murine colitis induced by DSS (n = 6). Severe colitis was induced by oral administration of DSS (2 w/v%) dissolved in drinking water for 7 days. Data represent the mean ± SEM for six mice per group. $^{*}P < 0.05$ versus vehicle-treated normal control group. $^{\#}P < 0.05$ compared to vehicle-treated DSS group.

3. Conclusion

Various ring-modified analogues of N-(5-hydroxy-3,4,6-trimethylpyridin-2-yl)acetamide (**9**) were synthesized in order to investigate the effects of ring structure on the anti-IBD activity. The results showed that either the trimethyl group or the hydroxyl group on the pyridine ring seem to play a critical role in the biological activities based on *in vitro* and *in vivo* models. The results that the dehydroxy analogue (**17**) and the detrimethyl analogue (**19**) are stronger than the parent compound (**9**) might provide an invaluable piece of information for the next generation anti-IBD agents. It also would be of great interest to investigate if the trend is valid in a side chain independent manner.

4. Experimental

4.1. Chemistry

General

Unless noted otherwise, materials were purchased from commercial suppliers and used without further purification. Air or moisture-sensitive reactions were carried out under an inert gas atmosphere. The reaction progress was monitored by thin layer-chromatography (TLC) using silica gel F_{254} plates. The products were purified by flash column chromatography using silica gel 60 (70–230 mesh) or by using the Biotage 'Isolera One' system with indicated solvents. Melting points were determined using a Fisher–Johns melting point apparatus and were not corrected. NMR spectra were obtained using a Bruker-250 spectrometer 250 MHz for ^{1}H-NMR, and 62.5 MHz for ^{13}C-NMR. Chemical shifts (δ) were expressed in ppm using a solvent as an internal standard and the coupling constant (J) in hertz. Low-resolution mass spectra (LRMS) were obtained using an Advion Expression CMS and recorded in a positive ion mode with an electrospray (ESI) source. High-resolution mass spectra (HRMS) were obtained using a

Finnigan LTQ Orbitrap mass spectrometer (Thermo Fisher Scientific Inc, MA, USA) operated in positive-ion electrospray mode.

6-Acetamido-2,4,5-trimethylpyridin-3-yl acetate (10)

To a suspension of *N*-(5-hydroxy-3,4,6-trimethylpyridin-2-yl)acetamide hydrochloride (**9**, 88 mg, 0.38 mmol) in acetone (2 mL) was added sodium acetate (110 mg, 1.15 mmol) and acetyl chloride (41 μL, 0.57 mmol) dropwise then stirred at room temperature for 3 h. The reaction mixture was diluted with EtOAc and H_2O, the aqueous layer was extracted with EtOAc. The combined EtOAc layer was dried over $MgSO_4$, filtered and, concentrated. The concentrated residue then purified by silica gel column chromatography (DCM/MeOH = 20/1) to afford **10** (71 mg, 79%). Pale yellow solid; TLC R_f 0.43 (DCM/MeOH = 9/1); m.p. 165 ℃; LRMS (ESI) *m/z* 237 $[M+H]^+$; ^1H NMR ($CDCl_3$) δ 8.62 (s, 1H), 2.35 (s, 3H), 2.28 (s, 3H), 2.16 (s, 3H), 2.14 (s, 3H), 2.10 (s, 3H); ^{13}C NMR ($CDCl_3$) δ 168.65 (2C), 146.71 (2C), 145.93, 143.34, 141.09, 23.48, 20.60, 18.94, 15.11, 13.47; HRMS (ESI) *m/z* calculated for $C_{12}H_{17}N_2O_3^+$ $[M+H]^+$ 237.1234, found 237.1236.

2-Acetamido-5-(benzyloxy)-3,4,6-trimethylpyridine 1-oxide (30)

To a solution of *N*-(5-(benzyloxy)-3,4,6-trimethylpyridin-2-yl)acetamide (**29**, 145 mg, 0.51 mmol) in $CHCl_3$ (5 mL) was added *m*-CPBA (106 mg, 0.61 mmol) and stirred at room temperature for 30 minutes. The reaction mixture was quenched with sodium sulfite solution, stirred at room temperature for additional 30 minutes and extracted with $CHCl_3$. The combined $CHCl_3$ layer was washed with sodium carbonate solution then dried over $MgSO_4$, filtered and, concentrated. The concentrated crude was purified by silica gel column chromatography (hexanes/EtOAc = 1/1 to EtOAc only) to afford **30** (179 mg, 97%). White solid; TLC R_f 0.48 (DCM/MeOH = 9/1); m.p. 162 ℃; LRMS (ESI) *m/z* 301 $[M+H]^+$; ^1H NMR ($CDCl_3$) δ 9.01 (s,

1H), 7.56–7.34 (m, 5H), 4.79 (s, 2H), 2.48 (s, 3H), 2.29 (s, 3H), 2.26 (s, 3H), 2.19 (s, 3H); ^{13}C NMR ($CDCl_3$) δ 169.44, 150.07, 141.17, 139.51, 136.01, 133.46, 128.93 (2C), 128.82, 128.21 (2C), 127.80, 76.13, 24.06, 16.37, 13.20, 12.30; HRMS (ESI) *m/z* calculated for $C_{17}H_{21}N_2O_3^+$ $[M+H]^+$ 301.1547, found 301.1536.

2-Acetamido-5-hydroxy-3,4,6-trimethylpyridine 1-oxide (11)

To a suspension of 2-acetamido-5-(benzyloxy)-3,4,6-trimethylpyridine 1-oxide (**30**, 50 mg, 0.17 mmol) in MeOH (3 mL) was added Pd/C (palladium, 10 wt.% on activated carbon, 10 mg) then stirred under hydrogen atmosphere at room temperature for 1 h. The reaction mixture was filtered through a pad of Celite and concentrated. The concentrated crude was purified by silica gel column chromatography (DCM/MeOH = 20/1) to afford **11** (28 mg, 80%). White solid; TLC R_f 0.24 (DCM/MeOH = 9/1); m.p. 206 ℃; LRMS (ESI) *m/z* 211 $[M+H]^+$; ^{1}H NMR (DMSO-d_6) δ 9.64 (s, 1H), 2.31 (s, 3H), 2.12 (s, 3H), 2.04 (s, 3H), 2.01 (s, 3H); ^{13}C NMR (DMSO-d_6) δ 169.11, 148.50, 135.34, 135.01, 128.27, 123.21, 22.62, 14.95, 12.40, 11.67; HRMS (ESI) *m/z* calculated for $C_{10}H_{15}N_2O_3^+$ $[M+H]^+$ 211.1077, found 211.1078.

2-Bromo-5-methoxy-3,4,6-trimethylpyridine (31)

To a suspension of 6-bromo-2,4,5-trimethylpyridin-3-ol (**25**, 200 mg, 0.93 mmol) in mixed THF-H_2O (1:1, 5 mL) solvent was added K_2CO_3 (1.3 g, 9.26 mmol) and iodomethane (288 μL, 4.63 mmol) at room temperature then stirred for 21 h. The reaction mixture was diluted with DCM and H_2O, the aqueous layer was extracted with DCM. The combined DCM layer was dried over $MgSO_4$, filtered and concentrated. The concentrated crude was purified by silica gel column chromatography (DCM only) to afford **31** (176 mg, 83%). Pale yellow solid; TLC R_f 0.40 (DCM/MeOH = 100/1); m.p. 38 ℃; LRMS (ESI) *m/z* 230 $[M+H]^+$; ^{1}H NMR ($CDCl_3$) δ 3.69 (s, 3H), 2.45 (s, 3H), 2.31 (s, 3H), 2.26 (s, 3H); ^{13}C NMR ($CDCl_3$) δ 152.90, 150.20,

141.42, 138.01 , 132.08, 60.45, 19.00, 18.90, 13.62; HRMS (ESI) *m/z* calculated for $C_9H_{13}BrNO^+$ $[M+H]^+$ 230.0175, found 230.0181.

_N_-(5-Methoxy-3,4,6-trimethylpyridin-2-yl)-1,1-diphenylmethanimine (32)

To a mixture of 2-bromo-5-methoxy-3,4,6-trimethylpyridine (**31**, 160 mg, 0.70 mmol) in toluene (5 mL) was added benzophenone imine (128 µL, 0.76 mmol), tris(dibenzylideneacetone)dipalladium $[Pd_2(dba)_3]$ (8 mg, 0.01 mmol), (*R*)-(+)-2,2'-bis(diphenylphosphino)-1,1'-binaphthalene (9 mg, 0.014 mmol) and sodium *tert*-butoxide (100 mg, 1.04 mmol) at room temperature and refluxed for 6 h. The reaction mixture was diluted with EtOAc and washed with brine. The EtOAc layer was dried over $MgSO_4$, filtered and concentrated. The concentrated crude was purified by silica gel column chromatography (Hex/EtOAc = 5/1) to afford **32** (221 mg, 96%). Pale yellow solid; TLC R_f 0.28 (hexanes/EtOAc = 4/1); m.p. 101 ℃; LRMS (ESI) *m/z* 331 $[M+H]^+$; ^{1}H NMR ($CDCl_3$) δ 7.80 (d, *J* = 7.3 Hz, 2H), 7.50–7.31 (m, 1H), 7.25–7.11 (m, 5H), 3.61 (dd, *J* = 2.2, 0.9 Hz, 3H), 2.31 (s, 3H), 2.09 (s, 3H), 1.92 (s, 3H); ^{13}C NMR ($CDCl_3$) δ 169.48, 157.07, 149.43, 146.91, 139.68, 139.35, 137.02, 130.92, 129.71 (2C), 129.01 (2C), 128.67, 128.10 (2C), 127.64 (2C), 119.69, 60.47, 18.85, 13.90, 12.48; HRMS (ESI) *m/z* calculated for $C_{22}H_{23}N_2O^+$ $[M+H]^+$ 331.1805, found 331.1818.

5-Methoxy-3,4,6-trimethylpyridin-2-amine (33)

To a mixture of *N*-(5-methoxy-3,4,6-trimethylpyridin-2-yl)-1,1-diphenylmethanimine (**32**, 100 mg, 0.30 mmol) in THF-MeOH (1:1, 5 mL) was added HCl in MeOH (2 M, 1.5 mL) dropwise and stirred at room temperature for 2 h. The reaction mixture was concentrated then the concentrated crude was diluted with EtOAc and saturated $NaHCO_3$ solution. The aqueous layer was extracted with EtOAc, the combined EtOAc layer dried over $MgSO_4$, filtered and

concentrated. The concentrated crude was then purified by silica gel column chromatography (DCM/MeOH = 30/1) to afford **33** (39 mg, 78%). Pale yellow solid; TLC R_f 0.60 (DCM/MeOH = 9/1); m.p. 92 ℃; LRMS (ESI) *m/z* 167 $[M+H]^+$; ^1H NMR ($CDCl_3$) δ 4.22 (s, 2H), 3.60 (s, 3H), 2.32 (s, 3H), 2.15 (s, 3H), 1.98 (s, 3H); ^{13}C NMR ($CDCl_3$) δ 152.38, 146.66, 145.86, 139.69, 113.54, 60.57, 18.55, 13.10, 12.46; HRMS (ESI) *m/z* calculated for $C_9H_{15}N_2O^+$ $[M+H]^+$ 167.1179, found 167.1182.

***N*-(5-Methoxy-3,4,6-trimethylpyridin-2-yl)acetamide (12)**

To a solution of 5-methoxy-3,4,6-trimethylpyridin-2-amine (**33**, 30 mg, 0.18 mmol) in DCM (2 mL) was added acetyl chloride (16 μL, 0.217 mmol) and triethylamine (75 μL, 0.54 mmol) at room temperature and stirred for 5 h. The reaction mixture was diluted with EtOAc and H_2O then extracted with EtOAc. The combined EtOAc layer was dried over $MgSO_4$, filtered and concentrated. The concentrated crude was then purified by silica gel column chromatography (DCM/MeOH = 50/1) to afford **12** (27.4 mg, 73%). Pale yellow solid; TLC R_f 0.19 (DCM/MeOH = 20/1); m.p. 109 ℃; LRMS (ESI) *m/z* 209 $[M+H]^+$; ^1H NMR ($CDCl_3$) δ 8.34 (s, 1H), 3.69 (s, 3H), 2.41 (s, 3H), 2.23 (s, 3H), 2.16 (s, 3H), 2.12 (s, 3H); ^{13}C NMR ($CDCl_3$) δ 169.57, 152.02, 147.80, 143.74, 141.51, 127.41, 60.39, 23.48, 18.75, 15.05, 12.98; HRMS (ESI) *m/z* calculated for $C_{11}H_{17}N_2O_2^+$ $[M+H]^+$ 209.1285, found 209.1289.

***N*-(5-Hydroxy-3,4-bis(hydroxymethyl)-6-methylpyridin-2-yl)acetamide (13)**

To a solution of 6-aminopyridoxine hydrochloride (**35**, 50 mg, 0.23 mmol) in acetic acid (230 μL) was added catalytic amount of sulfuric acid (5 μL) and acetic anhydride (65 μL, 0.69 mmol), and then stirred at 100 ℃ for 30 minutes. The reaction mixture was basified with saturated K_2CO_3 solution and concentrated. In concentrated crude, an excess amount of MeOH was added and undissolved solid was filtered off and then the filtrate was concentrated. The

concentrated crude was purified by silica gel column chromatography (DCM/MeOH = 20/1) to afford **13** (46 mg, 88%). Pale yellow solid; TLC R_f 0.32 (DCM/MeOH = 9/1); m.p. 292 ℃; LRMS (ESI) *m/z* 209 $[M+H–H_2O]^+$; ^{1}H NMR (DMSO-d_6) δ 10.06 (s, 1H), 4.93 (d, J = 1.7 Hz, 2H), 4.81 (s, 2H), 2.31 (s, 3H), 1.98 (s, 3H); ^{13}C NMR (DMSO-d_6) δ 167.64, 143.17, 143.08, 136.31, 135.93, 126.91, 72.33, 70.78, 22.75, 18.19; HRMS (ESI) *m/z* calculated for $C_{10}H_{15}N_2O_4^+$ $[M+H]^+$ 227.1026, found 227.1035.

***N*-(5-Hydroxy-3-(hydroxymethyl)-4,6-dimethylpyridin-2-yl)acetamide (14)**

To a solution of 6-amino-5-(hydroxymethyl)-2,4-dimethylpyridin-3-ol hydrochloride (**38**, 20 mg, 0.10 mmol) in acetic acid (250 μL) was added catalytic amount of sulfuric acid (5 μL) and acetic anhydride (28 μL, 0.30 mmol), and then stirred at 100 ℃ for 30 minutes. The reaction mixture was basified with saturated K_2CO_3 solution and concentrated. In concentrated crude, an excess amount of MeOH was added and undissolved solid was filtered off and then the filtrate was concentrated. The concentrated crude was purified by silica gel column chromatography (DCM/MeOH = 20/1) to afford **14** (10 mg, 48%). Pale yellow solid; TLC R_f 0.53 (DCM/MeOH = 9/1); m.p. 161 ℃; LRMS (ESI) *m/z* 211 $[M+H]^+$; ^{1}H NMR (DMSO-d_6) δ 9.76 (s, 1H), 8.70 (s, 1H), 4.58 (s, 1H), 4.29 (s, 2H), 2.31 (s, 3H), 2.24 (s, 3H), 2.00 (s, 3H); ^{13}C NMR (DMSO-d_6) δ 170.15, 148.11, 143.65, 140.05, 135.00, 128.66, 57.42, 22.69, 19.27, 12.13; HRMS (ESI) *m/z* calculated for $C_{10}H_{15}N_2O_3^+$ $[M+H]^+$ 211.1077, found 211.1079.

***N*-(5-(Benzyloxy)-4,6-dimethylpyrimidin-2-yl)acetamide (44)**

To a solution of 5-(benzyloxy)-4,6-dimethylpyrimidin-2-amine (**43**, 75 mg, 0.33 mmol) in DCM (2 ml) was added acetyl chloride (28 μL, 0.39 mmol) dropwise and triethylamine (137 μL, 0.98 mmol) then stirred at room temperature for 3 h. The reaction mixture was diluted with EtOAc and H_2O, extracted with EtOAc. The combined EtOAc layer was dried over $MgSO_4$,

filtered and concentrated. The concentrated crud was purified by silica gel column chromatography (hexanes/EtOAc = 4/1) to afford **44** (34 mg, 38%). White solid; TLC R_f 0.32 (hexanes/EtOAc = 1/1); m.p. 107 ℃; LRMS (ESI) *m/z* 272 $[M+H]^+$; ^{1}H NMR ($CDCl_3$) δ 8.41 (s, 1H), 7.46–7.33 (m, 5H), 4.81 (s, 2H), 2.46 (s, 3H), 2.39 (s, 6H); ^{13}C NMR ($CDCl_3$) δ 171.23, 161.69 (2C), 152.26, 146.34, 136.26, 128.84 (2C), 128.72, 128.28 (2C), 75.55, 24.98, 19.21 (2C); HRMS (ESI) *m/z* calculated for $C_{15}H_{18}N_3O_2^+$ $[M+H]^+$ 272.1394, found 272.1402.

***N*-(5-Hydroxy-4,6-dimethylpyrimidin-2-yl)acetamide (15)**

To a solution of *N*-(5-(benzyloxy)-4,6-dimethylpyrimidin-2-yl)acetamide (**44**, 30 mg, 0.11 mmol) in DCM (3 mL) was added pentamethylbenzene (49 mg, 0.33 mmol) and boron trichloride (1 M in DCM, 220 μL) dropwise at 0 ℃ and stirred at room temperature for 30 minutes. The reaction mixture was quenched with $CHCl_3$/MeOH (9/1, 5 mL) and stirred for additional 30 minutes. The reaction mixture was concentrated and, the concentrated crude was then purified by silica gel column chromatography (DCM/MeOH = 30/1) to afford **15** (9.8 mg, 49%). Pale yellow solid; TLC R_f 0.38 (DCM/MeOH = 20/1); m.p. 188 ℃; LRMS (ESI) *m/z* 182 $[M+H]^+$; ^{1}H NMR (DMSO-d_6) δ 10.02 (s, 1H), 8.87 (s, 1H), 2.31 (s, 6H), 2.07 (s, 3H); ^{13}C NMR (DMSO-d_6) δ 168.42, 154.33 (2C), 149.31, 143.72, 23.98, 18.82 (2C); HRMS (ESI) *m/z* calculated for $C_8H_{12}N_3O_2^+$ $[M+H]^+$ 182.0924, found 182.0919.

4-(Hydroxyimino)-2,3,6-trimethylcyclohexa-2,5-dien-1-one (47)

To a solution of trimethylhydroquinone (**45**, 400 mg, 2.60 mmol) in MeOH (3 mL) was added (diacetoxyiodo)benzene (931 mg, 2.90 mmol) suspended in MeOH (5 mL). The reaction mixture was stirred at room temperature for 1 h and solvent was evaporated. The residue was purified by silica gel column chromatography (Et_2O only) to give **46** as a yellow oil. Then, the purified **46** in THF (5 mL) was added hydroxylamine·HCl (740 mg, 10.65 mmol) followed by

addition of HCl (0.52 mL, 37% aqueous) and refluxed for 2 days. The reaction mixture was filtered, and the filtrate was concentrated. The concentrated crude was then purified by silica gel column chromatography (DCM/MeOH = 40/1) to afford **47** (309 mg, 72% for 2 steps). Yellow solid; TLC R_f 0.39 (DCM/MeOH = 20/1); m.p. 183 ℃; LRMS (ESI) *m/z* 166 $[M+H]^+$; ^{1}H NMR (DMSO-d_6) δ 13.10 (s, 1H), 7.56 (d, J = 1.5 Hz, 1H), 2.15 (d, J = 0.8 Hz, 3H), 1.93 (d, J = 1.5 Hz, 3H), 1.91 (d, J = 0.8 Hz, 3H); ^{13}C NMR (DMSO-d_6) δ 186.18, 149.09, 140.77, 137.42, 132.78, 120.54, 16.10, 12.95, 11.51; HRMS (ESI) *m/z* calculated for $C_9H_{12}NO_2^+$ $[M+H]^+$ 166.0863, found 166.0868.

4-Amino-2,3,6-trimethylphenol hydrochloride (48)

To a solution of 4-(hydroxyimino)-2,3,6-trimethylcyclohexa-2,5-dien-1-one (**47**, 100 mg, 0.61 mmol) in DCM (5 mL) were added tin(II) chloride dihydrate (413 mg, 1.83 mmol) and HCl (0.96 mL, 37% aqueous) then stirred at room temperature for 2 h. The reaction mixture was dissolved in excess amount of EtOAc, washed with $NaHCO_3$ solution and brine. The organic layer was dried over $MgSO_4$, filtered and concentrated. Then, 6 M HCl was added to the concentrated crude and stirred for 30 minutes, concentrated and vacuum dried to afford **48** (37.0 mg, 32%). Pale yellow solid; TLC R_f 0.58 (DCM/MeOH = 20/1); m.p. 287 ℃; LRMS (ESI) *m/z* 152 $[M+H–HCl]^+$; ^{1}H NMR (DMSO-d_6) δ 9.89 (s, 3H), 8.45 (s, 1H), 6.99 (s, 1H), 2.14 (s, 6H), 2.12 (s, 3H); ^{13}C NMR (DMSO-d_6) δ 152.52, 128.55, 125.00, 122.55, 122.12, 121.63, 16.52, 13.89, 12.61; HRMS (ESI) *m/z* calculated for $C_9H_{14}NO^+$ $[M–Cl]^+$ 152.1070, found 152.1067.

***N*-(4-Hydroxy-2,3,5-trimethylphenyl)acetamide (16)**

To a suspension of 4-amino-2,3,6-trimethylphenol hydrochloride (**48**, 24 mg, 0.13) in acetone (2 ml) was added sodium acetate (14 mg, 0.17 mmol) and acetyl chloride (11 μL, 0.15 mmol)

dropwise at room temperature, stirred for 3 h then diluted with EtOAc and H_2O. The aqueous layer was extracted with EtOAc. The combined EtOAc layer was dried over $MgSO_4$, filtered and, concentrated. The concentrated residue was dissolved in a small amount of EtOAc then added hexane for precipitation. The precipitate was collected by filtration and dried to afford **16** (10.3 mg, 41%). White solid; TLC R_f 0.26 (DCM/MeOH = 20/1); m.p. 212 ℃; LRMS (ESI) *m/z* 194 $[M+H]^+$; ^1H NMR (DMSO-d_6) δ 9.11 (s, 1H), 7.98 (s, 1H), 6.74 (s, 1H), 2.09 (d, *J* = 3.5 Hz, 6H), 1.97 (s, 6H); ^{13}C NMR (DMSO-d_6) δ 168.59, 151.11, 130.62, 128.42, 126.17, 123.76, 121.84, 23.35, 16.98, 14.95, 13.25; HRMS (ESI) *m/z* calculated for $C_{11}H_{16}NO_2^+$ $[M+H]^+$ 194.1176, found 194.1165.

2-Bromo-3,4,6-trimethyl-5-((1-phenyl-1*H*-tetrazol-5-yl)oxy)pyridine (50)

To a suspension of 6-bromo-2,4,5-trimethylpyridin-3-ol (**25**, 1.1 g, 5.10 mmol) in CH_3CN (10 mL) was added 5-chloro-1-phenyl-1*H*-tetraole (968 mg, 5.36 mmol) and NaOH (205 mg, 5.13 mmol) then allowed to react on microwave reactor at 200 W, 100 ℃ for 1 h. The reaction mixture was quenched and diluted with ice H_2O then the precipitate was filtered, washed with ice H_2O and collected. The collected precipitate was vacuum dried to afford **50** (1.7 g, 92%). White solid; m.p. 156 ℃; LRMS (ESI) *m/z* 360 $[M+H]^+$; ^1H NMR ($CDCl_3$) δ 7.89–7.80 (m, 2H), 7.68–7.51 (m, 3H), 2.39 (s, 3H), 2.37 (s, 3H), 2.20 (s, 3H); ^{13}C NMR ($CDCl_3$) δ 158.90, 148.42, 147.44, 141.65, 140.33, 133.31, 133.07, 130.12 (2C), 129.87, 121.98 (2C), 19.21, 19.05, 14.25.

1,1-Diphenyl-*N*-(3,4,6-trimethyl-5-((1-phenyl-1*H*-tetrazol-5-yl)oxy)pyridin-2-yl)methanimine (51)

To a mixture of 2-bromo-3,4,6-trimethyl-5-((1-phenyl-1*H*-tetrazol-5-yl)oxy)pyridine (**50**, 1.7 g, 4.72 mmol) in toluene (15 mL) was added benzophenone imine (871 μL, 5.19 mmol),

tris(dibenzylideneacetone)dipalladium [$Pd_2(dba)_3$] (98 mg, 0.09 mmol), (*R*)-(+)-2,2'-bis(diphenylphosphino)-1,1'-binaphthalene (118 mg, 0.19 mmol) and sodium *tert*-butoxide (907 mg, 9.44 mmol) at room temperature then refluxed for 3 h. The reaction mixture was diluted with EtOAc and washed with brine. The EtOAc layer was dried over $MgSO_4$, filtered and concentrated. The concentrated crude was dried to afford **51** and used in next step without further purification. Pale yellow solid; TLC R_f 0.33 (Hex/EtOAc = 2/1); m.p. 181 ℃; LRMS (ESI) *m/z* 461 $[M+H]^+$; ^1H NMR ($CDCl_3$) δ 7.84 (d, *J* = 7.9 Hz, 4H), 7.67–7.45 (m, 4H), 7.47–7.09 (m, 7H), 2.22 (s, 3H), 2.04 (s, 3H), 2.01 (s, 3H); ^{13}C NMR ($CDCl_3$) δ 169.92, 159.79, 159.42, 145.43, 144.27, 139.00, 138.72, 136.66, 133.33, 131.23, 129.98 (4C), 129.83, 129.56 (2C), 128.96, 128.04 (d, *J* = 16.1 Hz), 121.96 (4C), 120.79 (2C), 19.14, 13.97, 13.14; HRMS (ESI) *m/z* calculated for $C_{28}H_{25}N_6O^+$ $[M+H]^+$ 461.2084, found 461.2065.

3,4,6-Trimethyl-5-((1-phenyl-1*H*-tetrazol-5-yl)oxy)pyridin-2-amine (52)

To a crude 1,1-diphenyl-N-(3,4,6-trimethyl-5-((1-phenyl-1*H*-tetrazol-5-yl)oxy)pyridin-2-yl)methanimine (**51**) in THF-MeOH (1:1, 10 mL) was added HCl in MeOH (2 M, 10 mL) dropwise and stirred at room temperature for 3 h. The reaction mixture was concentrated then the concentrated crude was washed with EtOAc and vacuum dried to afford **52** (979 mg, 70% for 2 steps). Beige solid; TLC R_f 0.36 (DCM/MeOH = 40/1); m.p. 224 ℃; LRMS (ESI) m/z 297 $[M+H]^+$; ^1H NMR ($CDCl_3$) δ 7.97–7.79 (m, 2H), 7.68–7.48 (m, 3H), 4.44 (s, 2H), 2.23 (s, 3H), 2.09 (s, 3H), 2.04 (s, 3H); ^{13}C NMR ($CDCl_3$) δ 159.78, 154.93, 144.63, 141.50, 138.08, 133.26, 129.94 (2C), 129.50 (2C), 121.84, 113.99, 18.96, 13.21, 13.10; HRMS (ESI) *m/z* calculated for $C_{15}H_{17}N_6O^+$ $[M+H]^+$ 297.1458, found 297.1465.

3,4,6-Trimethylpyridin-2-amine (53)

To a mixture of 3,4,6-trimethyl-5-((1-phenyl-1*H*-tetrazol-5-yl)oxy)pyridin-2-amine (**52**, 100

mg, 0.34 mmol) in MeOH (5 mL) was added Pd/C (palladium, 10 wt.% on activated carbon, 20 mg) then the mixture was stirred under hydrogen atmosphere at room temperature for 3 days. The reaction mixture was filtered through pad of Celite and the filtrate was concentrated. The concentrated crude was purified by silica gel column chromatography (DCM/MeOH = 40/1) to afford **53** (23 mg, 51%). White solid; TLC R_f 0.36 (DCM/MeOH = 9/1); m.p. 110 ℃; LRMS (ESI) *m/z* 137 $[M+H]^+$; ^{1}H NMR (DMSO-d_6)) δ 6.37 (s, 1H), 6.20 (s, 2H), 2.22 (s, 3H), 2.15 (s, 3H), 1.95 (s, 3H); ^{13}C NMR (DMSO-d_6) δ 155.81, 148.37, 147.86, 114.08, 112.43, 21.27, 19.47, 11.81; HRMS (ESI) *m/z* calculated for $C_8H_{13}N_2^+$ $[M+H]^+$ 137.1073, found 137.1079.

_N_-(3,4,6-trimethylpyridin-2-yl)acetamide (17)

To a suspension of 3,4,6-trimethylpyridin-2-amine (**53**, 28 mg, 0.21 mmol) in acetone (2 mL) was added sodium acetate (51 mg, 0.62 mmol) and acetyl chloride (18 μL, 0.25 mmol) dropwise then stirred at room temperature for 4 h. The reaction solvent was concentrated, concentrated crude was diluted with DCM and saturated $NaHCO_3$ solution and, extracted with DCM. The combined DCM layer was dried over $MgSO_4$, filtered and, concentrated. The concentrated residue was then purified by silica gel column chromatography (DCM/MeOH = 9/1) to afford **17** (9.5 mg, 25%). Pale yellow solid; TLC R_f 0.44 (DCM/MeOH = 9/1); m.p. 122 ℃; LRMS (ESI) *m/z* 179 $[M+H]^+$; ^{1}H NMR ($CDCl_3$) δ 9.17 (s, 1H), 6.85 (s, 1H), 2.39 (s, 3H), 2.26 (s, 3H), 2.16 (s, 3H), 2.12 (s, 3H); ^{13}C NMR ($CDCl_3$) δ 169.79, 153.66, 149.11, 148.73, 125.39, 123.38, 23.40, 23.25, 20.04, 14.19; HRMS (ESI) *m/z* calculated for $C_{10}H_{15}N_2O^+$ $[M+H]^+$ 179.1179, found 179.1184.

5-Bromo-3,4,6-trimethylpyridin-2-amine (54)

To a solution of 3,4,6-trimethylpyridin-2-amine (**53**, 15 mg, 0.11 mmol) in acetonitrile (1 mL)

were added ammonium acetate (1.5 mg, 0.02 mmol) and portion wise *N*-bromosuccinimide (23 mg, 0.13 mmol) at 0 ℃. The reaction mixture was stirred at 0 ℃ for 10 minutes then concentrated. The concentrated crude was diluted with EtOAc and H_2O and, extracted with EtOAc. The combined EtOAc layer was dried over $MgSO_4$, filtered and concentrated. The concentrated crude was purified by silica gel column chromatography (hexanes/EtOAc = 5/1) to afford **54** (9.6 mg, 41%). Yellow solid; TLC R_f 0.44 (Hex/EtOAc = 1/1); m.p. 154 ℃; LRMS (ESI) m/z 215 $[M+H]^+$; ^1H NMR ($CDCl_3$) δ 4.32 (s, 2H), 2.50 (s, 3H), 2.36 (s, 3H), 2.09 (s, 3H); ^{13}C NMR ($CDCl_3$) δ 154.89, 152.06, 145.75, 113.88, 113.83, 25.48, 20.23, 13.99; HRMS (ESI) *m/z* calculated for $C_8H_{12}BrN_2^+$ $[M+H]^+$ 215.0178, found 215.0182.

***N*-(5-Bromo-3,4,6-trimethylpyridin-2-yl)acetamide (18)**

To a mixture of 5-bromo-3,4,6-trimethylpyridin-2-amine (**54**, 9 mg, 0.042 mmol) in acetone (1 mL) was added triethylamine (18 μL, 0.13 mmol) and acetyl chloride (4 μL, 0.054 mmol) dropwise, the mixture was stirred at room temperature for 24 h then reaction solvent was concentrated. The concentrated residue was diluted with EtOAc and H_2O. The aqueous layer was extracted with EtOAc. The combined EtOAc layer was dried over $MgSO_4$, filtered and, concentrated. The concentrated crude was purified by silica gel column chromatography (EtOAc only) to afford **18** (5.1 mg, 47%). White solid; TLC R_f 0.43 (EtOAc only); m.p. 147 ℃; LRMS (ESI) *m/z* 257 $[M+H]^+$; ^1H NMR ($CDCl_3$) δ 7.89 (s, 1H), 2.59 (s, 3H), 2.44 (s, 3H), 2.20 (s, 6H); ^{13}C NMR ($CDCl_3$) δ 169.76, 153.22, 148.69, 146.70, 122.50, 119.66, 25.44, 23.71, 20.76, 16.02; HRMS (ESI) *m/z* calculated for $C_{10}H_{14}BrN_2O^+$ $[M+H]^+$ 257.0284, found 257.0290.

4.2. Biology

Cell culture

Human colonic epithelial cell line, HT-29, human colon epithelial cell line, CCD-841, and human pre-monocytic cell line, U937, were obtained from the American Type Culture Collection (Manassas, VA, USA). Cells were cultured in RPMI-1640 media containing 10% FBS, 100 IU/mL of penicillin and 100 µg/mL of streptomycin, and maintained at 37 ℃ in 5% CO_2 in a humidified incubator.

Monocyte-epithelial cell adhesion assay

Adhesion of monocytes to colon epithelial cells was determined by using U937 pre-monocytic human cells prelabeled with 2′,7′- bis(carboxyethyl)-5(6′)-carboxyfluorescein acetoxymethyl ester (BCECF/AM, 10 µg/mL) as previously reported [24,25] with slight modification. HT-29 cells (2×10^5 cells/well) cultured in 48-well plates were pretreated with compounds for 1 h. The prelabeled U937 cells were centrifuged and then seeded (5×10^5 cells/well) on the monolayer of HT-29 cells and the co-culture was treated with TNF-α (10 ng/mL) for 3 h at 37 ℃. Non-adhering U937 cells were removed by washing thrice with PBS. Cells were lysed with 0.1% Triton X-100 in Tris (0.1 M) in a shaker for 30 minutes at room temperature. The fluorescence intensity was then measured using Fluostar Optima microplate reader (BMG LABTECH GmbH, Germany) at an excitation and emission wavelengths of 485 and 520 nm, respectively.

Cytotoxicity measurement (MTT assay)

The normal human colon epithelial cell line, CCD-841, was used to measure cytotoxic effects of compounds and tofacitinib. Cells were seeded in 96-well plates and treated with or without drugs in media containing 1% FBS for 48 h. Then, 3-(4,5-dimethylthiazol-2-yl)-2,5-diphenyl tetrazolium bromide (MTT) was added to the wells. After 4 hours of forming formazan crystal, DMSO was added, and absorbance was measured at 540 nm using a Fluostar Optima microplate reader.

Chick chorioallantoic membrane (CAM) model of angiogenesis

Angiogenesis was examined using the previously published methods [40,57]. VEGF (20 ng/CAM) or TNF-α (20 ng/CAM) was dissolved in PBS containing 0.1% bovine serum albumin (BSA) and added topically to the sterile disk on top of nine-day-old chick embryo CAMs. Compound **17**, **19** or vehicle was then applied topically to the CAMs. The CAM tissue directly beneath the disk was resected from the embryo after 72 h and harvested under light microscopy (Leica, Wetzlar, Germany). The number of new blood vessel branch points contained in a circular region equal to the area of the filter disk was then counted for each section. Inhibition ratio (%) of compounds was calculated according to equation 1.

Angiogenesis inhibition ratio (%) = ([B]–[A])/[B]×100 (equation 1)

where [A] and [B] represent angiogenesis after a three-day incubation with TNF-α in the presence or absence of test compounds, respectively.

DSS-induced colitis in mice

C57BL/6N/Crl female mice were used for generation of DSS-induced colitis. Control mice were given normal drinking water throughout the study period, while mice in experimental groups were given 2w/v% DSS (MW 36–50 KDa; MP Biomedicals, Solon, OH, USA) solution as drinking water for 6 days (n = 5). In another set of experiments, DSS treatment continued for 7 days (n = 6). Drinking bottles were changed every third day. Body weights, stool consistencies, and the presence of fecal blood were recorded daily. Drugs and compounds were administered daily starting at 6th day after DSS treatment and continued for 7 days. At the end of the experiments, mice were sacrificed by CO_2 inhalation.

Animal experiment ethics

The study protocol of the animal experiment was reviewed and approved beforehand by the Institutional Animal Care and Use Committee of Yeungnam University and were performed following the institutional guidelines of the Institute of Laboratory Animal Resources (1996), and of Yeungnam University for the care and use of animals (2009).

Measurement of MPO

MPO (myeloperoxidase) levels were measured in homogenized colon tissues. Briefly, colon tissue (50 mg) was mixed with 300 μL lysis buffer and homogenized using a Bead blaster 24 (Benchmark Scientific, NJ, USA). MPO levels in collected supernatants were determined using an MPO Assay Kit (Hycult Biotech, Uden, Netherlands).

Statistics

Statistical significances between groups were determined using one-way or two-way ANOVA followed by the Student-Newman-Keul comparison method (GraphPad Prism 5.0 software, San Diego, CA, USA). Results are presented as the means ± standard errors of at least three independent experiments. Statistical significance was accepted for p values < 0.05.

Acknowledgement

This study was supported by a grant of the Korean Health Technology R&D Project, Ministry of Health & Welfare, Republic of Korea (HI15C0542).

References

[1]. E. Langholz, Current trends in inflammatory bowel disease: the natural history, Ther. Adv. Gastroenterol. 3 (2010) 77–86.

https://doi.org/10.1177/1756283X10361304.

[2]. H.S. De Souza, C. Fiocchi, Immunopathogenesis of IBD: current state of the art, Nat. Rev. Gastroenterol. Hepatol. 13 (2016) 13–27. https://doi.org/10.1038/nrgastro.2015.186.

[3]. D.C. Baumgart, W.J. Sandborn, Crohn's disease, Lancet 380 (2012) 1590–1605. https://doi.org/10.1016/S0140-6736(12)60026-9.

[4]. H. Akiho, A. Yokoyama, S. Abe, Y. Nakazono, M. Murakami, Y. Otsuka, K. Fukawa, M. Esaki, Y. Niina, H. Ogino, Promising biological therapies for ulcerative colitis: A review of the literature. World J. Gastrointest. Pathophysiol. 6 (2015) 219–227. https://doi.org/10.4291/wjgp.v6.i4.219.

[5]. GBD 2017 inflammatory bowel disease collaborators, The global, regional, and national burden of inflammatory bowel disease in 195 countries and territories, 1990-2017: a systematic analysis for the Global Burden of Disease Study 2017, Lancet Gastroenterol. Hepatol. 5 (2020) 17–30. https://doi.org/10.1016/S2468-1253(19)30333-4

[6]. K.L. Wallace, L.-B. Zheng, K. Yoshitake, D.Q. Shih, Immunopathology of inflammatory bowel disease, World J. Gastroenterol. 20 (2014) 6–21. https://doi.org/10.3748/wjg.v20.i1.6.

[7]. Y. Huang, Z. Chen, Inflammatory bowel disease related innate immunity and adaptive immunity, Am. J. Transl. Res. 8 (2016) 2490–2497.

[8]. E. Giraudo, L. Primo, E. Audero, H.P. Gerber, P. Koolwijk, S. Soker, M. Klagsbrun, N. Ferrara, F.J. Bussolino, Tumor necrosis factor-α regulates expression of vascular endothelial growth factor receptor-2 and of its co-receptor neuropilin-1 in human vascular endothelial cells, J. Biol Chem. 273 (1998) 22128–22135. https://doi.org/10.1074/jbc.273.34.22128.

[9]. N. Parameswaran, S. Patial, Tumor necrosis factor-α signaling in macrophages, Crit. Rev. Eukaryot. Gene Expr. 20 (2010) 87–103. https://doi.org/10.1615/critreveukargeneexpr.v20.i2.10.

[10]. E.A. Carswell, L.J. Old, R.L. Kassel, S. Green, N. Fiore, B. Williamson., An endotoxin-induced serum factor that causes necrosis of tumors, Proc. Natl. Acad. Sci. U S A. 72 (1975) 3666–3670. https://doi.org/10.1073/pnas.72.9.3666.

[11]. K.E. Porter, N.A. Turner, D.J. O'Regan, S.G. Ball, Tumor necrosis factor α induces human atrial myofibroblast proliferation, invasion and MMP-9 secretion: inhibition by simvastatin, Cardiovasc. Res. 64 (2004) 507–515. https://doi.org/10.1016/j.cardiores.2004.07.020.

[12]. Y. Zheng, L. Sun, T. Jiang, D. Zhang, D. He, H. Nie, TNFα promotes Th17 cell differentiation through IL-6 and IL-1β produced by monocytes in rheumatoid arthritis, J. Immunol. Res. 2014 (2014) 385352. https://doi.org/10.1155/2014/385352.

[13]. C. Monaco, J. Nanchahal, P. Taylor, M. Feldmann, Anti-TNF therapy: past, present and future, Int. Immunol. 27 (2015) 55–62. https://doi.org/10.1093/intimm/dxu102.

[14]. T. Ali, S. Kaitha, S. Mahmood, A. Ftesi, J. Stone, M.S. Bronze, Clinical use of anti-TNF therapy and increased risk of infections, Drug Healthc. Patient Saf. 5 (2013) 79–99. https://doi.org/10.2147/DHPS.S28801.

[15]. W.J. Sandborn, New targets for small molecules in inflammatory bowel disease, Gastroenterol Hepatol. 11 (2015) 338–340.

[16]. P. Olivera, S. Danese, L. Peyrin-Biroulet, Next generation of small molecules in inflammatory bowel disease, Gut 66 (2016) 199–209. https://doi.org/10.1136/gutjnl-2016-312912.

[17]. J. Sabino, B. Verstockt, S. Vermeire, M. Ferrante, New biologics and small molecules in inflammatory bowel disease: an update, Therap. Adv. Gastroenterol. 12 (2019) 1756284819853208. https://doi.org/10.1177/1756284819853208.

[18]. K.S. Currie, L. Patel, K.F. Sedillo, Small-molecule agents for the treatment of inflammatory bowel disease, Bioorg. Med. Chem. Lett. 29 (2019) 2034–2041. https://doi.org/10.1016/j.bmcl.2019.06.042.

[19]. S. Dhillon, Tofacitinib: a review in rheumatoid arthritis, Drugs. 77 (2017) 1987–2001. https://doi.org/10.1007/s40265-017-0835-9.

[20]. A. Fernández-Clotet, J. Castro-Poceiro, J. Panés, Tofacitinib for the treatment of ulcerative colitis, Expert Rev. Clin. Immunol. 14 (2018) 881–892. https://doi.org/10.1080/1744666X.2018.1532291.

[21]. J. Panés, W.J. Sandborn, S. Schreiber, B.E. Sands, S. Vermeire, G. D'Haens, R. Panaccione, P.D.R. Higgins, J.F. Colombel, B.G. Feagan, G. Chan, M. Moscariello, W. Wang, W. Niezychowski, A. Marren, P. Healey, E. Maller, Tofacitinib for induction and maintenance therapy of Crohn's disease: results of two phase IIb randomised placebo-controlled trials, Gut 66 (2017) 1049–1059. https://doi.org/10.1136/gutjnl-2016-312735.

[22]. J. Panés, G.R. D'Haens, P.D.R. Higgins, L. Mele, M. Moscariello, G. Chan, W. Wang, W. Niezychowski, C. Su, E. Maller, Long-term safety and tolerability of oral tofacitinib in patients with Crohn’s disease: results from a phase 2, open-label, 48-week extension study, Aliment. Pharmacol. Ther. 49 (2019) 265–276. https://doi.org/10.1111/apt.15072.

[23]. M.F. Neurath, Current and emerging therapeutic targets for IBD, Nat. Rev. Gastroenterol. Hepatol. 14 (2017) 269–278. https://doi.org/10.1038/nrgastro.2016.208.

[24]. D. Thapa, J.S. Lee, S.Y. Park, Y.H. Bae, S.K. Bae, J.B. Kwon, K.J. Kim, M.K. Kwak, Y.J. Park, H.G. Choi, J.A. Kim, Clotrimazole ameliorates intestinal inflammation and abnormal angiogenesis by inhibiting interleukin-8 expression through a nuclear factor-κB-dependent manner, J. Pharmacol. Exp. Ther. 327 (2008) 353–364. https://doi.org/10.1124/jpet.108.141887.

[25]. D. Thapa, J.S. Lee, M.A. Park, M.Y. Cho, Y.J. Park, H.G. Choi, T.C. Jeong, J.A. Kim, Inhibitory effects of clotrimazole on TNF-α-induced adhesion molecule expression and angiogenesis, Arch. Pharm. Res. 32 (2009) 593–603. https://doi.org/10.1007/s12272-009-1416-6.

[26]. J.D. Sedgwick, D.S. Riminton, J.G. Cyster, H. Körner, Tumor necrosis factor: a master-regulator of leukocyte movement, Immunol. Today 21 (2000) 110–113. https://doi.org/10.1016/s0167-5699(99)01573-x.

[27]. Z.g. Liu, Molecular mechanism of TNF signaling and beyond, Cell Res. 15 (2005) 24e27. https://doi.org/ 10.1038/sj.cr.7290259.

[28]. S.Y. Park, S.K. Ku, E.S. Lee, J.A. Kim, 1,3-Diphenylpropenone ameliorates TNBS-induced rat colitis through suppression of NF-κB activation and IL-8 induction, Chem. Biol. Interact. 196 (2012) 39–49. https://doi.org/10.1016/j.cbi.2012.02.002.

[29]. S. Park, S.C. Regmi, S.Y. Park, E.K. Lee, J.H. Chang, S.K. Ku, D.H. Kim, J.A. Kim, Protective effect of 7-O-succinyl macrolactin A against intestinal inflammation is mediated through PI3-kinase/Akt/mTOR and NF-κB signaling pathways, Eur. J. Pharmacol. 735 (2014) 184–192. https://doi.org/10.1016/j.ejphar.2014.04.024.

[30]. S. Banskota, H.E. Kang, D.G. Kim, S.W. Park, H. Jang, U. Karmacharya, B.S. Jeong, J.A. Kim, T.G. Nam, In vitro and in vivo inhibitory activity of 6-amino-

2,4,5-trimethylpyridin-3-ols against inflammatory bowel disease, Bioorg. Med. Chem. Lett. 26 (2016) 4587–4591. https://doi.org/10.1016/j.bmcl.2016.08.075.

[31]. T.M. Kadayat, S. Banskota, P. Gurung, G. Bist, T.B.T. Magar, A. Shrestha, J.A. Kim, E.S. Lee, Discovery and structure-activity relationship studies of 2-benzylidene-2,3-dihydro-1H-inden-1-one and benzofuran-3(2H)-one derivatives as a novel class of potential therapeutics for inflammatory bowel disease, Eur. J. Med. Chem. 8 (2017) 575–597. https://doi.org/10.1016/j.ejmech.2017.06.018.

[32]. P. Gurung, S. Banskota, N. Katila, J. Gautam, T.M. Kadayat, D.Y. Choi, E.S. Lee, T.C. Jeong, J.A. Kim, Ameliorating effect of TI-1-162, a hydroxyindenone derivative, against TNBS-induced rat colitis is mediated through suppression of RIP/ASK-1/MAPK signaling, Eur. J. Pharmacol. 827 (2018) 94–102. https://doi.org/10.1016/j.ejphar.2018.03.027.

[33]. S.W. Park, S. Banskota, P. Gurung, Y.J. Jin, H.E. Kang, C.L. Chaudhary, S.Y. Lee, B.S. Jeong, J.A. Kim, T.G. Nam, Synthesis and evaluation of 6-heteroarylamino-2,4,5-trimethylpyridin-3-ols as inhibitors of TNF-α-induced cell adhesion and inflammatory bowel disease, MedChemComm. 9 (2018) 1305–1310. https://doi.org/10.1039/c8md00156a.

[34]. T.M. Kadayat, S. Banskota, G. Bist, P. Gurung, T.B.T. Magar, A. Shrestha, J.A. Kim, E.S. Lee, Synthesis and biological evaluation of pyridine-linked indanone derivatives: Potential agents for inflammatory bowel disease, Bioorg. Med. Chem. Lett. 28 (2018) 2436–2441. https://doi.org/10.1016/j.bmcl.2018.06.012.

[35]. C.L. Chaudhary, P. Gurung, S. Jang, S. Banskota, T.G. Nam, J.A. Kim, B.S. Jeong, Synthesis, activity and mechanism of alkoxy-, carbamato-, sulfonamido-, thioureido-, and ureido-derivatives of 2,4,5-trimethylpyridin-3-ol against inflammatory bowel disease, J. Enzyme Inhib. Med. Chem. 35 (2020) 1–20.

https://doi.org/10.1080/14756366.2019.1677637.

[36]. R. Serwa, T.G. Nam, L. Valgimigli, S. Culbertson, C.L. Rector, B.S. Jeong, D.A. Pratt, N.A. Porter, Preparation and investigation of vitamin B6-derived aminopyridinol antioxidants, Chem. Eur. J. 16 (2010) 14106–14114. https://doi.org/10.1002/chem.201001382.

[37]. D.G. Kim, Y. Kang, H. Lee, E.K. Lee, T.G. Nam, J.A. Kim, B.S. Jeong, 6-Amino-2,4,5-trimethylpyridin-3-ols: A new general synthetic route and antiangiogenic activity, Eur. J. Med. Chem., 78 (2014) 126–139. https://doi.org/10.1016/j.ejmech.2014.03.045.

[38]. H. Lee, S. Banskota, D.G. Kim, J.H. Been, Y.J. Jin, J. Gautam, H. Jang, T.G. Nam, J.A. Kim, B.S. Jeong, Synthesis and antiangiogenic activity of 6-amido-2,4,5-trimethylpyridin-3-ols, Bioorg. Med. Chem. Lett. 24 (2014) 3131–3136. https://doi.org/10.1016/j.bmcl.2014.05.005.

[39]. S. Banskota, J. Gautam, S.C. Regmi, P. Gurung, M.H. Park, S.J. Kim, T.G. Nam, B.S. Jeong, J.A. Kim, BJ-1108, a 6-amino-2,4,5-trimethylpyridin-3-ol analog, inhibits serotonin-induced angiogenesis and tumor growth through PI3K/NOX pathway, PLoS ONE, 11 (2016) e0148133. https://doi.org/10.1371/journal.pone.0148133.

[40]. J. Gautam, S. Banskota, S.C. Regmi, S. Ahn, Y.H. Jeon, H. Jeong, S.J. Kim, T.G. Nam, B.S. Jeong, J.A. Kim, Tryptophan hydroxylase 1 and 5-HT7 receptor preferentially expressed in triple-negative breast cancer promote cancer progression through autocrine serotonin signaling, Mol. Cancer, 15 (2016) 75. https://doi.org/10.1186/s12943-016-0559-6.

[41]. M. Timilshina, Y. Kang, I. Dahal, Z. You, T.G. Nam, K.J. Kim, B.S. Jeong, J.H. Chang, BJ-3105, a 6-alkoxypyridin-3-ol analog, impairs T cell differentiation and

prevents experimental autoimmune encephalomyelitis disease progression, PLoS ONE, 12 (2017) e0168942. https://doi.org/10.1371/journal.pone.0168942.

[42]. Y. Kang, M. Timilshina, T.G. Nam, B.S. Jeong, J.H. Chang, BJ-1108, a 6-amino-2,4,5-trimethylpyridin-3-ol analogue, regulates differentiation of Th1 and Th17 cells to ameliorate experimental autoimmune encephalomyelitis, Biol. Res. 50 (2017) 8. https://doi.org/10.1186/s40659-017-0113-z.

[43]. Z. You, M. Timilshina, B.S. Jeong, J.H. Chang, BJ-2266 ameliorates experimental autoimmune encephalomyelitis through down-regulation of the JAK/STAT signaling pathway, Eur. J. Immunol. 47 (2017) 1488−1500. https://doi.org/10.1002/eji.201646860.

[44]. D. Bae, J. Gautama, H. Jang, S. Banskota, S.Y. Lee, M.J. Jeong, A.S. Kim, H.C. Kim, I.H. Lee, T.G. Nam, J.A. Kim, B.S. Jeong, Protective effects of 6-ureido/thioureido-2,4,5-trimethylpyridin-3-ols against 4-hydroxynonenal-induced cell death in adult retinal pigment epithelial-19 cells, Bioorg. Med. Chem. Lett. 28 (2018) 107–112. https://doi.org/10.1016/j.bmcl.2017.11.046.

[45]. S. Acharya, M. Timilshina, L. Jiang, S. Neupane, D.Y. Choi, S.W. Park, S.Y. Lee, B.S. Jeong, J.A. Kim, T.G. Nam, J.H. Chang, Amelioration of Experimental autoimmune encephalomyelitis and DSS induced colitis by NTG-A-009 through the inhibition of Th1 and Th17 cells differentiation, Sci. Rep. 8 (2018) 7799. https://doi.org/10.1038/s41598-018-26088-y.

[46]. J. Gautam, S. Banskota, P. Chaudhary, S. Dahal, D.G. Kim, H.E. Kang, I.H. Lee, T.G. Nam, B.S. Jeong, J.A. Kim, Antitumor activity of BJ-1207, a 6-amino-2,4,5-trimethylpyridin-3-ol derivative, in human lung cancer, Chem. Biol. Interact. 294 (2018) 1−8. https://doi.org/10.1016/j.cbi.2018.08.007.

[47]. J.H. Chidlow Jr, D. Shukla, M.B. Grisham, C.G. Kevil, Pathogenic angiogenesis in

IBD and experimental colitis: new ideas and therapeutic avenues, Am. J. Physiol. Gastrointest. Liver Physiol. 293 (2007) G5−G18. https://doi.org/10.1152/ajpgi.00107.2007.

[48]. A. Diamanti, T. Capriati, B. Papadatou, D. Knafelz, F. Bracci, T. Corsetti, D. Elia, G. Torre, The clinical implications of thalidomide in inflammatory bowel diseases, Expert Rev. Clin. Immunol. 11 (2015) 699−708. https://doi.org/10.1586/1744666X.2015.1027687.

[49]. S.M. Culbertson, G.D. Enright, K.U. Ingold, Synthesis of a novel radical trapping and carbonyl group trapping anti-AGE agent: a pyridoxamine analogue for inhibiting advanced glycation (AGE) and lipoxidation (ALE) end products, Org Lett. 5 (2003) 2659−2962. https://doi.org/10.1021/ol0348147.

[50]. T.G. Nam, J.M. Ku, C.L. Rector, H. Choi, N.A. Porter, B.S. Jeong, Pyridoxine-derived bicyclic aminopyridinol antioxidants: synthesis and their antioxidant activities, Org. Biomol. Chem. 9 (2011) 8475–8482. https://doi.org/10.1039/c1ob05144j.

[51]. B. Roschek, K.A. Tallman, C.L. Rector, J.G. Gillmore, D.A. Pratt, C. Punta, N.A. Porter, Peroxyl radical clocks, J Org Chem. 71 (2006) 3527–3532. https://doi.org/10.1021/jo0601462.

[52]. Y.T. Han, G.I. Choi, D. Son, N.J. Kim, H. Yun, S. Lee, D.J. Chang, H.S. Hong, H. Kim, H.J. Ha, Y.H. Kim, H.J. Park, J. Lee, Y.G. Suh, Ligand-based design, synthesis, and biological evaluation of 2-aminopyrimidines, a novel series of receptor for advanced glycation end products (RAGE) inhibitors, J Med Chem. 55 (2012) 9120–9135. https://doi.org/10.1021/jm300172z.

[53]. L.I. Smith, W.B. Irwin, The structures of arylhydrazones of unsymmetrically substituted quinones, J. Am. Chem. Soc. 63 (1941) 1036–1043.

https://doi.org/10.1021/ja01849a042.

[54]. R.A.W. Johnstone, P.J. Price, Metal-assisted reactions: part 19. Burst kinetics in heterogeneous catalytic transfer hydrogenolysis, J. Chem. Soc., Perkin Trans. 1 (1987) 1069–1076. https://doi.org/10.1039/P19870001069

[55]. M.A. Ashwell, W.R. Solvibile, S. Han, E. Largis, R. Mulvey, J. Tillet, 4-Aminopiperidine ureas as potent selective agonists of the human beta(3)-adrenergic receptor, Bioorg. Med. Chem. Lett. 11 (2001) 3123–3127. https://doi.org/10.1016/s0960-894x(01)00645-x.

[56]. R.C. Sainson, D.A. Johnston, H.C. Chu, M.T. Holderfield, M.N. Nakatsu, S.P. Crampton, J. Davis, E. Conn, C.C. Hughes, TNF primes endothelial cells for angiogenic sprouting by inducing a tip cell phenotype, Blood 111 (2008) 4997–5007. https://doi.org/10.1182/blood-2007-08-108597.

[57]. B.C. Park, D. Thapa, J.S. Lee, S.Y. Park, J.A. Kim, Troglitazone inhibits vascular endothelial growth factor-induced angiogenic signaling via suppression of reactive oxygen species production and extracellular signal-regulated kinase phosphorylation in endothelial cells, J. Pharmacol. Sci. 111 (2009) 1–12. https://doi.org/10.1254/jphs.08305fp.

Graphical abstract

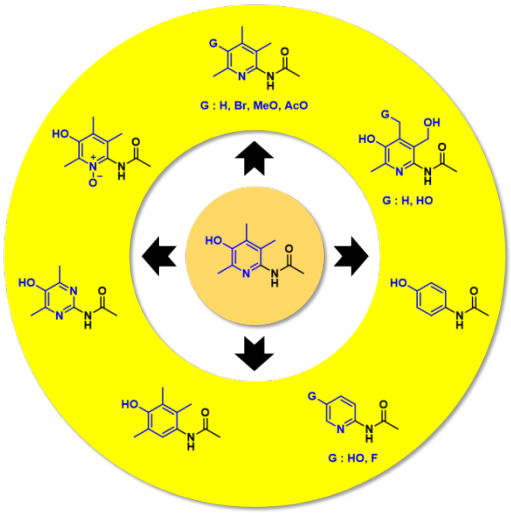

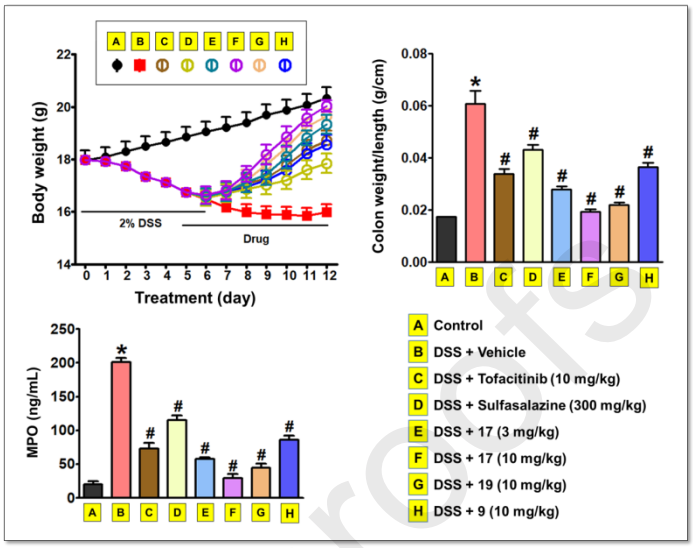

Highlights

- Ring-modified analogues of 6-acetamido-2,4,5-trimethylpyridin-3-ol were synthesized
- Structure-activity relationship of the ring-modified analogues were established
- Compound **17** inhibited TNF-α-induced responses in colonic epithelial cells better than tofacitinib
- Anti-colitis efficacy of compound **17** was much greater than tofacitinib in mice

Declaration of interests

☒ **The authors declare that they have no known competing financial interests or personal relationships that could have appeared to influence the work reported in this paper.**

☐ The authors declare the following financial interests/personal relationships which may be considered as potential competing interests: